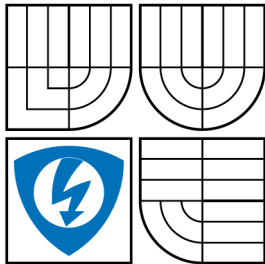


BRNO UNIVERSITY OF TECHNOLOGY  
VYSOKÉ UČENÍ TECHNICKÉ V BRNĚ



FACULTY OF ELECTRICAL ENGINEERING AND  
COMMUNICATION  
DEPARTMENT OF TELECOMMUNICATIONS

FAKULTA ELEKTROTECHNIKY A KOMUNIKAČNÍCH  
TECHNOLOGIÍ  
ÚSTAV TELEKOMUNIKACÍ

## DESIGN OF GENERALIZED POWERTRAIN MODEL

MASTER'S THESIS  
DIPLOMOVÁ PRÁCE

AUTHOR  
AUTOR PRÁCE

Bc. TOMÁŠ BORKOVEC

SUPERVISOR  
VEDOUČÍ PRÁCE

doc. Ing. VLADISLAV ŠKORPIL, CSc.

BRNO 2015



VYSOKÉ UČENÍ  
TECHNICKÉ V BRNĚ

Fakulta elektrotechniky  
a komunikačních technologií

Ústav telekomunikací

# Diplomová práce

magisterský navazující studijní obor  
Telekomunikační a informační technika

**Student:** Bc. Tomáš Borkovec

**ID:** 134456

**Ročník:** 2

**Akademický rok:** 2014/2015

**NÁZEV TÉMATU:**

## Design of Generalized Powertrain Model

### POKYNY PRO VYPRACOVÁNÍ:

Propose generalized powertrain model, identify correct yet simple sub-model for engines and energy sources. Find way to express usable energy in all on-board energy sources, must use same unit. For given route on road-network compute optimal charge/torque splitting ratios. Process IGN terrain data and OSM maps data to produce three dimensional road network map of Ile-de-France. Compute energy demand profile for any given road.

### DOPORUČENÁ LITERATURA:

[1] Guzzella, L. - Sciarretta, A. Vehicle Propulsion Systems, Introduction to Modelling and Optimization, Second Edition. 2007.

[2] Rousseau, G. Véhicule Hybride et Commande Optimale. Th

**Termín zadání:** 9.2.2015

**Termín odevzdání:** 26.5.2015

**Vedoucí práce:** doc. Ing. Vladislav Škorpil, CSc.

**Konzultanti diplomové práce:**

**doc. Ing. Jiří Mišurec, CSc.**

*Předseda oborové rady*

### UPOZORNĚNÍ:

Autor diplomové práce nesmí při vytváření diplomové práce porušit autorská práva třetích osob, zejména nesmí zasahovat nedovoleným způsobem do cizích autorských práv osobnostních a musí si být plně vědom následků porušení ustanovení § 11 a následujících autorského zákona č. 121/2000 Sb., včetně možných trestněprávních důsledků vyplývajících z ustanovení části druhé, hlavy VI. díl 4 Trestního zákoníku č.40/2009 Sb.

## **ABSTRACT**

In this work is proposed the generalized powertrain of the parallel hybrid car. The powertrain is composed from the sub-models of the power sources. Each sub-model is described by the quasi-static modeling. For given routes is computed the power demand. Based on the derived power demand, three energy management systems are tested. First system is based on heuristic rules. The second one use more sophisticated control algorithms - the optimization method. Main idea is based on minimum principle, when the control algorithm tries to minimize the cost function (fuel use, emission). The last one is based on the equivalent consumption minimization strategy.

## **KEYWORDS**

Hybrid electric vehicle, internal combustion engine, electric motor, energy optimalisation, quasi-static modeling

## **ABSTRAKT**

V této práci je popsán obecný model paralelního hybridního automobilu. Celkový hnací systém je složen z menších sub-systémů popsaných pomocí kvazi-statického modelování. Pro dané cesty je vypočítána potřebná síla pro pohon vozidla po trase. Na základě znalosti požadované síly jsou testovány tři řídicí systémy. První je založen na heuristických pravidlech. Druhý je založen na optimalizaci dané funkce jenž představuje výslednou spotřebu nebo množství vytvořených emisí. Třetí systém je založen na metodě ECMS.

## **KLÍČOVÁ SLOVA**

Hybridní elektrické vozidlo, spalovací motor, elektrický motor, energetická optimalizace, kvazi-statické modelování

BORKOVEC, Tomáš *DESIGN OF GENERALIZED POWERTRAIN MODEL*: master's thesis. Brno: Brno University of Technology, Faculty of Electrical Engineering and Communication, Department of Telecommunications, 2015. 58 p. Supervised by doc. Ing. Vladislav Škorpil, CSc.

## DECLARATION

I declare that I have written my master's thesis on the theme of "DESIGN OF GENERALIZED POWERTRAIN MODEL" independently, under the guidance of the master's thesis supervisor and using the technical literature and other sources of information which are all quoted in the thesis and detailed in the list of literature at the end of the thesis.

As the author of the master's thesis I furthermore declare that, as regards the creation of this master's thesis, I have not infringed any copyright. In particular, I have not unlawfully encroached on anyone's personal and/or ownership rights and I am fully aware of the consequences in the case of breaking Regulation § 11 and the following of the Copyright Act No 121/2000 Sb., and of the rights related to intellectual property right and changes in some Acts (Intellectual Property Act) and formulated in later regulations, inclusive of the possible consequences resulting from the provisions of Criminal Act No 40/2009 Sb., Section 2, Head VI, Part 4.

Brno .....

.....

(author's signature)

## ACKNOWLEDGEMENT

My sincere thanks goes to prof. Ing. František Zezulka, CSc. for offering me the internship opportunities in foreign university. Then, I would like to express my gratitude to my supervisor doc. Ing. Vladislav Škorpil, CSc. for the support of my study, for his patience, motivation, enthusiasm, and immense knowledge.

Brno .....

.....

(author's signature)



ESIEE Paris  
Cité Descartes - BP 99  
2 boulevard Blaise Pascal  
93162 Noisy le Grand  
France  
<http://www.esiee.fr>

## ACKNOWLEDGEMENT

Work described in this master's thesis has been implemented in the laboratories supported by the ESIEE university. I would like to express my gratitude to professor Arben Cela for supervising of this work. Also, I would like to thank to student Ing. Matěj Kubička for the useful comments, remarks and engagement through the learning process of this master thesis.

Brno .....

.....

(author's signature)



Faculty of Electrical Engineering  
and Communication  
Brno University of Technology  
Purkynova 118, CZ-61200 Brno  
Czech Republic  
<http://www.six.feec.vutbr.cz>

## ACKNOWLEDGEMENT

Research described in this bachelor's thesis has been implemented in the laboratories supported by the SIX project; reg. no. CZ.1.05/2.1.00/03.0072, operational program Výzkum a vývoj pro inovace.

Místo .....

.....

author's signature



EVROPSKÁ UNIE  
EVROPSKÝ FOND PRO REGIONÁLNÍ ROZVOJ  
INVESTICE DO VAŠÍ BUDOUCNOSTI



# CONTENTS

<b>Introduction</b>	<b>11</b>
<b>1 Hybrid electric car modeling</b>	<b>12</b>
1.1 Degree of hybridization . . . . .	12
1.2 Hybrid electric vehicle architecture . . . . .	13
1.3 Parallel HEV operating modes . . . . .	15
1.3.1 Classification . . . . .	17
1.4 Basic car model . . . . .	17
1.4.1 One dimensional movement . . . . .	17
1.4.2 Longitudinal dynamic model . . . . .	18
1.5 Components . . . . .	20
1.5.1 IC engine . . . . .	20
1.5.2 Electric motor . . . . .	21
1.5.3 Battery . . . . .	22
<b>2 Energy management</b>	<b>26</b>
2.1 Classifications of control strategies . . . . .	26
2.1.1 Rule-based control strategies . . . . .	26
2.1.2 Optimization-based control strategies . . . . .	27
2.2 Drive cycle . . . . .	28
2.3 Rule-based control strategy in parallel hybrid vehicle . . . . .	32
2.4 Equivalent consumption minimization strategy . . . . .	37
<b>3 Conclusion</b>	<b>48</b>
<b>Bibliography</b>	<b>49</b>
<b>List of symbols, physical constants and abbreviations</b>	<b>52</b>
<b>List of appendices</b>	<b>54</b>
<b>A Appendix 1</b>	<b>55</b>
<b>B Content of attached CD</b>	<b>58</b>



# LIST OF FIGURES

1.1	Degree of hybridization . . . . .	13
1.2	Series hybrid . . . . .	14
1.3	Parallel hybrid . . . . .	14
1.4	Series-Parallel hybrid . . . . .	15
1.5	Power assist mode . . . . .	15
1.6	Regenerative braking mode . . . . .	16
1.7	Battery recharged mode . . . . .	16
1.8	Conventional vehicle mode . . . . .	16
1.9	Zero emission mode . . . . .	16
1.10	Forces acting on a vehicle in motion . . . . .	18
1.11	Quasistatic model of the ICE . . . . .	20
1.12	ICE efficiency map with maximum torque curve (thick line) . . . . .	21
1.13	Quasistatic model of the EM . . . . .	22
1.14	Efficiency map for the electric motor. The thick lines represent maximal torque for given speed . . . . .	23
1.15	Quasistatic model of the Battery . . . . .	23
1.16	Equivalent circuit of battery . . . . .	24
1.17	Variation discharge and charge resistance in dependency on SOC . . . . .	25
1.18	Variation of the voltage $V_{oc}$ in dependency on SOC . . . . .	25
2.1	The road in map given by vertices and edges . . . . .	28
2.2	Speed profile for given road . . . . .	30
2.3	Power profile for given road . . . . .	30
2.4	Speed profile for New European Driving Cycle . . . . .	31
2.5	Power profile for New European Driving Cycle . . . . .	32
2.6	Speed profile for FTP-75 . . . . .	32
2.7	Power profile for FTP-75 driving cycle . . . . .	33
2.8	ICE efficiency map with operating points. . . . .	34
2.9	Flowchart for $0.55 < \text{Batt\_SOC} < 0.7$ . . . . .	35
2.10	SOC variations for FTP-75 driving cycle . . . . .	36
2.11	Engine efficiency map with operating points . . . . .	36
2.12	Power trajectory in fuel path for FTP-75 driving cycle . . . . .	37
2.13	Power trajectory in electrical path for FTP-75 driving cycle . . . . .	37
2.14	Offline ECMS flow chart . . . . .	40
2.15	SOC variations for FTP-75 driving cycle . . . . .	41
2.16	SOC variations for FTP-75 driving cycle . . . . .	42
2.17	SOC variations for FTP-75 driving cycle . . . . .	42
2.18	The graph of $\bar{E}_f = f(\bar{E}_e)$ for FTP-75 drive cycle . . . . .	44

- 2.19 The ECMS flowchart . . . . . 45
- 2.20 SOC variations for FTP-75 driving cycle . . . . . 46
- 2.21 Power trajectory in fuel path for FTP-75 driving cycle . . . . . 46
- 2.22 Power trajectory in electrical path for FTP-75 driving cycle . . . . . 47
- A.1 Flowchart for  $0.55 < \text{Batt\_SOC} < 0.7$  . . . . . 55
- A.2 Flowchart for  $\text{Batt\_SOC} < 0.55$  . . . . . 56
- A.3 Flowchart for  $0.55 < \text{Batt\_SOC} < 0.57$  & flag = true . . . . . 57

# INTRODUCTION

The total number of vehicles in the World is growing every year and we consider using personal cars for transportation people or belongings as a standard thing. The traffic on the roads is composed mainly from a vehicles with a conventional propulsion - the internal combustion engine. With growing number of vehicles also grows the consumption of fossil fuels and the emission. The fuel consumption is one of the main issue in automobile production. Due to low level of fossil fuel were introduced an alternative power sources (fuel cell, natural gas, propane) and different powertrain architectures. Nowadays there is big pressure to achieve the lowest possible fuel consumption. It leads to downsizing the engines, but on the other side is a customer which asks good performance and comfort.

The hybrid electric vehicles (HEV) offer the possibility to achieve both. The HEVs can reduce the consumption of fuel and increase energy security, because they use electric-drive technologies to boost efficiency. Secondly, they do not pollute environmental. They produce less, in a case of the parallel hybrid vehicles, or zero, in a case of pure electric vehicles, tailpipe emissions. HEV could be classified with respect to the level of hybridization into several groups. The electric vehicles use the large battery pack to store the electric energy which power the electric motor. The batteries are charged during the regenerative braking or from an external power source. Second group use drivetrain with two power sources. Vehicle is propelled by the internal combustion engine, that use energy saved in fuel, and by the electric motor, that use energy saved in batteries.

In this work is used the model from second group-the parallel hybrid vehicle. The primary source is the combustion engine. Extra power from the electric motor gives a possibility to use smaller engines in powertrain. To charge the batteries the vehicle use regenerative braking, when the motor acts as a generator and store the energy into the batteries or the combustion engine.

The firs part deals with the architecture of hybrid electric vehicles, introduces the division based on a degree of hybridization. In case of parallel HEV are described the particular modes in which the vehicle can acts during the drive. Than the mathematical description of vehicle is derived. Last section of this part describes the main components in powertrain, the characteristics and quasi-static models.

In second part the power management techniques are discussed. The driving cycles are introduced and the power profiles are computed. Based on derived power profiles three control techniques are tested. One from the rule-based control strategy and two from the optimization-based control strategy.

# 1 HYBRID ELECTRIC CAR MODELING

The main idea of Hybrid Electric Vehicle (HEV) is possibility to combine the advantages of an electrical vehicles (EV) and a vehicles with internal combustion engine (ICE) together. This connection should positively affect poor fuel economy, environmental pollution and dissipation of vehicle kinetic energy during braking compared to ICE vehicles. The HEV also have wider operation range in compare with purely EV. In principle, it is possible to[1]:

- downsize the engine and still fulfill the maximum power requirements of the vehicle,
- recover some energy during deceleration,
- optimize the power distribution between parallel power sources,
- eliminate the idle fuel consumption by turning off the engine when no power is required,
- eliminate the clutching losses by engaging the engine only when the speeds match.

In fact, not all the point mentioned above are used simultaneously, also the weight of HEVs is about 10-30 % higher than the conventional vehicles[1]. The hybrid electric vehicle use two prime movers the internal combustion engine and the electrical motor, but can be extended by another electrical motor (generator).

## 1.1 Degree of hybridization

The conception to use two or more energy conversion machines opens a wide area of possibilities how to combine this power sources. Also the size of each machine can be changed to fulfill designer's ideas. First of all is important to define if the vehicle will be ICE dominated or EM dominated. ICE-dominated vehicles have internal combustion engine as a primary propulsion system and relatively small electric motor with a battery pack. In a case of EM-dominated HEVs an electric motor is a principal propulsion unit which use an energy saved in a large battery pack. In such an architecture the ICE will be used to charge the batteries. This decision defines the configuration (serial, parallel) of the vehicle. To quantify the level of domination of an HEV, the concept of degree of hybridization (DOH) has been developed (Fig.1.1). The DOH is a number between 0–1 which represents the ratio of the maximum power output of two or more power sources defined as 1.1.[12]

$$DOH = 1 - \frac{|P_{max,ED1} - P_{max,ED2}|}{P_{max,ED1} + P_{max,ED2}}, \quad (1.1)$$

where  $ED1$  and  $ED2$  are two different energy conversion devices. For specific HEV architecture with one ICE with nominal power output  $P_{ICE\_max}$  and one EM with

nominal power output  $P_{EM\_max}$ , the DOH can be written as

$$DOH = 1 - \frac{|P_{EM\_max} - P_{ICE\_max}|}{P_{EM\_max} + P_{ICE\_max}}. \quad (1.2)$$

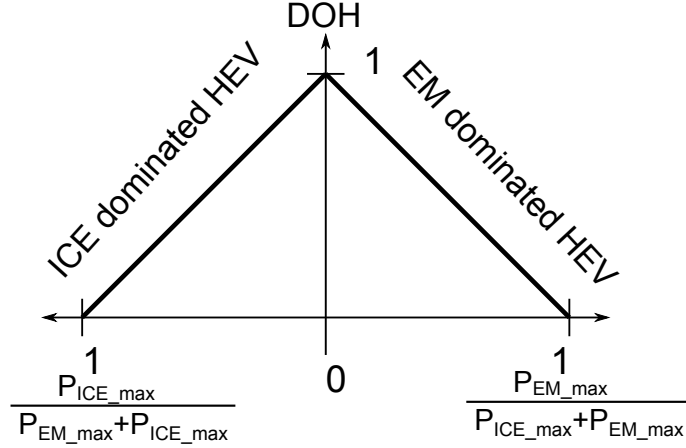


Fig. 1.1: Degree of hybridization

## 1.2 Hybrid electric vehicle architecture

Classification of Hybrid electric vehicle is defined by a connection between the single components inside the drivetrain, this also determines the energy flow. The HEV are divided in three main groups:

- Series hybrid
- Parallel hybrid
- Series-parallel hybrid

### Series HEVs

Series hybrid propulsion systems use single traction electric motor to propel the vehicle. Electric energy can be supplied by battery or by internal combustion engine. The ICE output is converted by generator into electricity that can feeds directly the electric motor or charge the battery pack (Fig 1.2). This architecture enables to the engine operates at a point with the optimal efficiency and emissions, because engine does not propel the vehicle directly. The regenerative braking and the transmission does not require clutch. During regenerative braking the traction motor acts as a generator and charge the battery. The fact that the energy from the engine is converted two times and that the series HEV needs three machines (ICE, electric motor and generator) decreases the over all efficiency of this architecture.

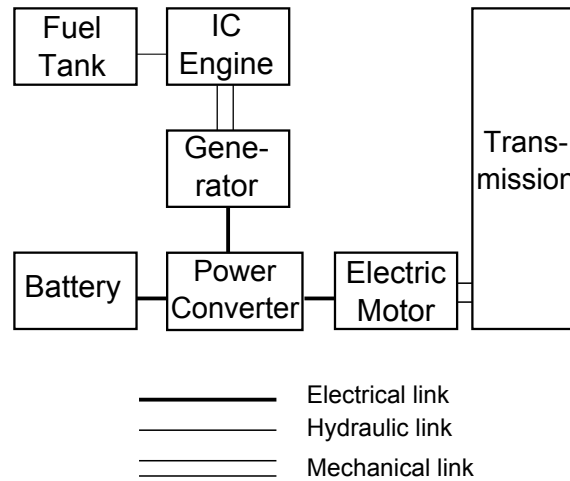


Fig. 1.2: Series hybrid

### Parallel HEVs

Parallel hybrid vehicle uses for driving two prime movers - the internal combustion engine and the electric motor (Fig 1.3). Usually the ICE supply traction power and its assisted by electric engine. In fact both machines can drive the vehicle alone or in combination. Significant advantage is possibility to the control power distribution between two parallel paths. The combustion engine can be turned off during idle and the electric motor can assist during acceleration or driving non-horizontal way. There is no need to use third energy converter as a generator to charge the battery, because this role takes the electric motor during braking or during driving with only use the ICE.

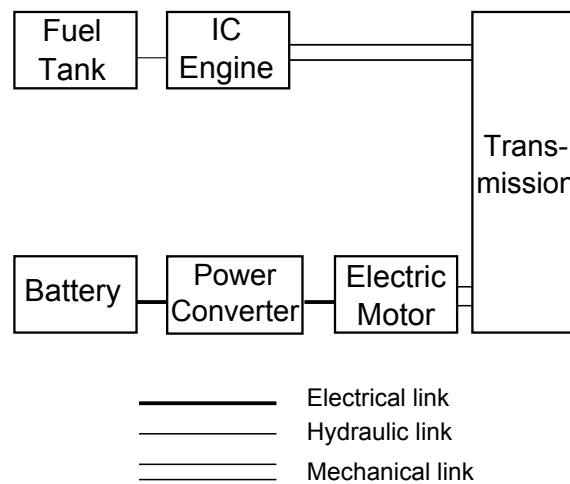


Fig. 1.3: Parallel hybrid

## Series-parallel HEVs

This system combines two architectures presented above together. The HEV utilizes three energy converters in total. One combustion engine and one electric motor are prime movers which propel the vehicle. The third machine works as a generator in a series hybrid system to charge the battery.

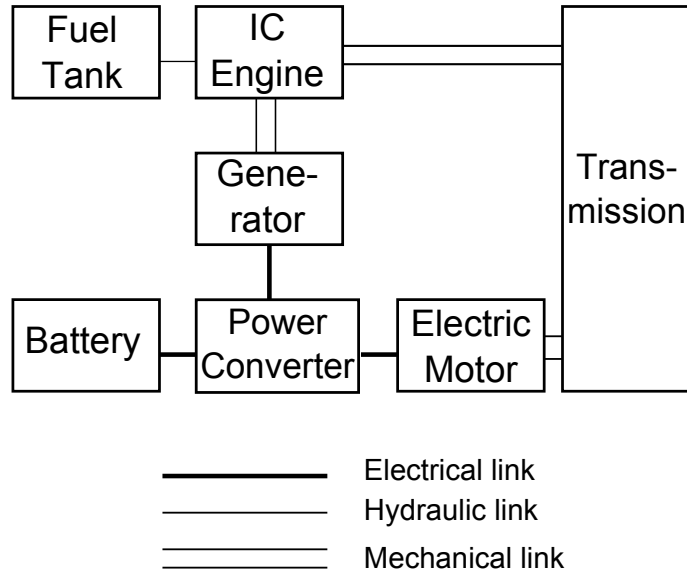


Fig. 1.4: Series-Parallel hybrid

## 1.3 Parallel HEV operating modes

In the parallel hybrid vehicles is the internal combustion engine and the electrical motor mechanically connected in torque coupler. This device also combines the torque from both ways. Clearly there is need to use the control unit that will regulate the power distribution. The control signal determines the operating mode for each component in a powertrain. During the startup or acceleration is used the power assist mode, when the engine provides only some part of total demanded power, the rest is delivered by the motor (Fig. 1.5).[1]. During braking or deceleration the

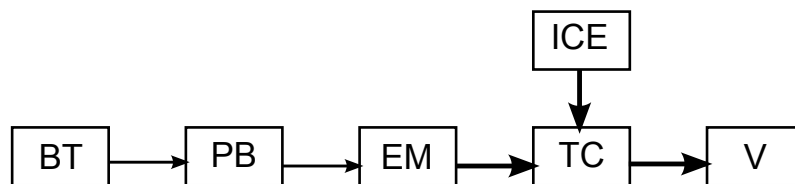


Fig. 1.5: Power assist mode

motor works in generator mode and recuperates energy into the battery pack(Fig. 1.6). The engine can charge the battery during driving in the mode with light load.

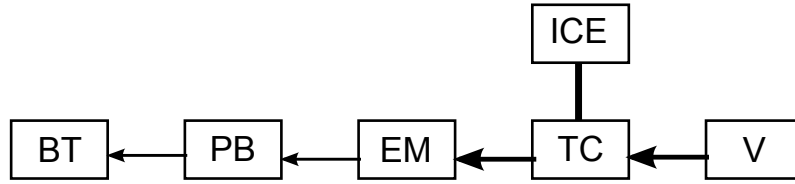


Fig. 1.6: Regenerative braking mode

The ICE provides more power than is required. The extra power is used to charge the battery through the motor (Fig. 1.7). Pure engine operation is used when

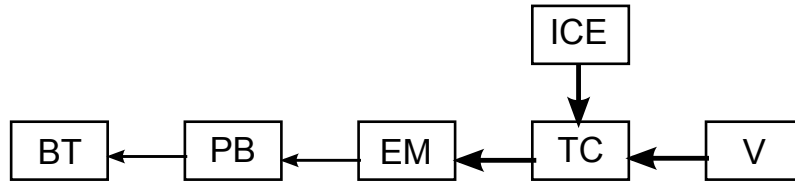


Fig. 1.7: Battery recharged mode

the battery is completely depleted, than the EM can not work in traction mode. Also when the demanded torque at the wheel is in optimal efficiency are the ICE can propel the vehicle alone.(Fig. 1.8). Pure motor operation are also possible in

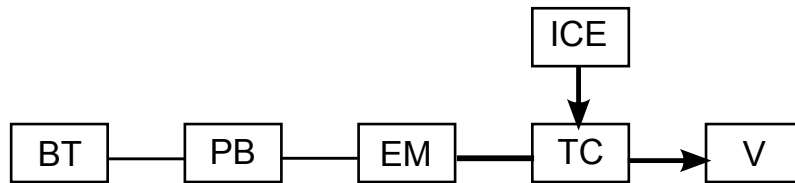


Fig. 1.8: Conventional vehicle mode

situation, where the engine cannot operate effectively, like zero emission or very low speed driving (Fig. 1.9).

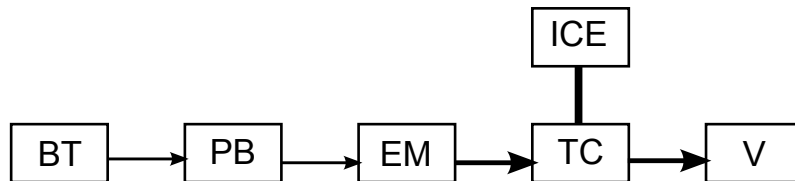


Fig. 1.9: Zero emission mode



### 1.3.1 Classification

The parallel hybrid electric vehicles can be further classified in terms of degree of hybridization[1].

- Micro hybrid—the drivetrain is based on the internal combustion engine as a primary power source with an additional small electric motor. There is no need for a high capacity battery neither a complex power electronic.
- Mid hybrid—the power delivered by the electric motor is sufficient for engine boosting but not for driving whole vehicle. The EM transfer the energy from regenerative braking into battery.
- Full hybrid—use all operating modes-power assist, energy recuperation and pure electric motor operation. For this reasons is used such an electric motor which can deliver sufficient power to drive the vehicle alone.

## 1.4 Basic car model

Main goal of this work is to implement control which will effectively split demanded power between two parallel ways. First step is to obtain demanded energy to drive the vehicle over the driving cycle. In this section is introduced a general description of vehicle movement.

### 1.4.1 One dimensional movement

To describe the forces acting on the moving vehicle, is this act simplified to one-dimensional movement as shown in the figure 1.10. Behavior of a vehicle driving exact direction is given by all forces acting on this direction. According to the Newton's second law, vehicle acceleration can be written as

$$\frac{dV}{dt} = \frac{\sum F_t - \sum F_r}{\delta M} \quad (1.3)$$

where  $V$  is vehicle speed,  $\sum F_t$  is total tractive effort of the vehicle,  $\sum F_r$  is total resistance,  $M$  is the total mass of a vehicle and  $\delta$  is mass factor for converting the rotational inertias of rotating components into translation mass.

Vehicle resistance is composed from the rolling resistance  $F_r$  (which includes the rolling resistance of the front and rear wheels), the wind resistance  $F_w$ , the climbing resistance  $F_g$  (caused by gravity during driving uphill). Against this forces acts the total tractive effort  $F_t$ (composed from the traction effort of the front and rear tires) this force is generated by the prime mover (can be negative in case of braking) minus force used for accelerate the rotating parts and all friction losses in the powertrain [1]. By developing the equation 1.3 we obtain the dynamic equation

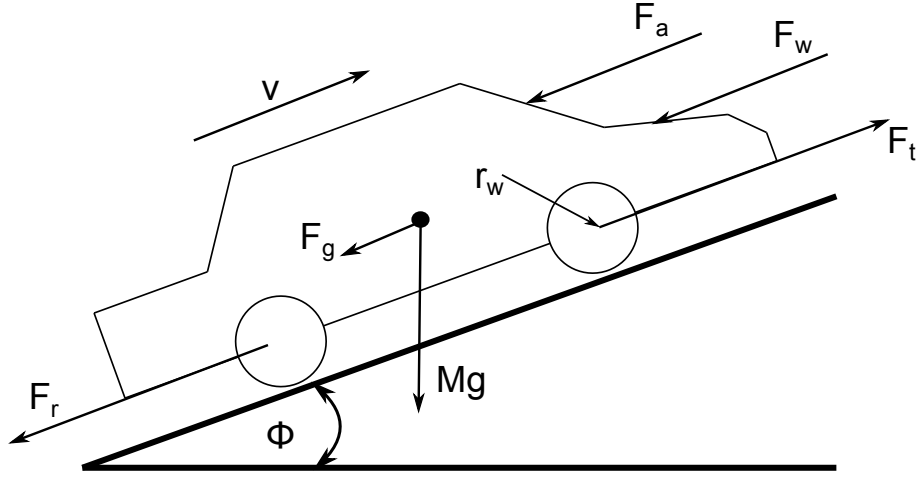


Fig. 1.10: Forces acting on a vehicle in motion

for the longitudinal dynamic model in the form:

$$M \frac{dV}{dt} = F_t - (F_r + F_w + F_g) \quad (1.4)$$

When a vehicle is driving along well known way the amount of mechanical energy spend by a vehicle mainly depends on three effects [1]:

- the aerodynamic friction losses
- the rolling friction losses
- the energy scattered during braking

### 1.4.2 Longitudinal dynamic model

The longitudinal model of vehicle is based on vehicle multi-body dynamic as shown in figure 1.10.

#### Rolling resistance

The rolling resistance force can modeled as:

$$F_r(v, p, \dots) = c_r(v, p, \dots) \times M \times g \times \cos(\phi), \quad v > 0, \quad (1.5)$$

where  $M$  is the vehicle total mass,  $g$  is the gravity acceleration,  $\cos(\phi)$  models the influence of non-horizontal road and  $c_r$  is the rolling friction coefficient, which depends on many variables. Mainly vehicle speed  $v$ , tire pressure  $p$  and road surface conditions. The influence of tire pressure is approximately corresponding to  $\frac{1}{\sqrt{p}}$ . A wet road can increase  $c_r$  by 20%, and driving in extreme condition can double this value.[10]

## Wind resistance

The wind resistance, acts on vehicle in motion is composed by viscous friction of the surrounding air on the vehicle surface and by the pressure difference between the front and rear of the vehicle. For standard passenger car, the body causes approximately 65% of the aerodynamic resistance. The rest is due to wheel housing, exterior mirrors, window housing and the engine ventilation. To compute the wind resistance, the vehicle is simplifying to a prismatic body with a frontal area  $A_f$ . The force caused by stagnation pressure is multiplied by an aerodynamic drag coefficient  $c_d$ . [1]

$$F_w(v) = \frac{1}{2} \times \rho \times A_f \times c_d \times v^2 \quad (1.6)$$

where  $v$  is the vehicle speed,  $\rho$  is the density of the ambient air.

## Climbing Resistance

It is the conservative force inducted by gravity when driving non-horizontal road.

$$F_g(\phi) = M \times g \times \sin(\phi) \quad (1.7)$$

where  $M$  is the total vehicle mass,  $g$  the acceleration due to gravity,  $\phi$  is road angle, if the angle is small can be replaced by grade value as

$$\sin(\phi) \approx \tan(\phi) = \frac{h}{l} \quad (1.8)$$

where  $h$  is achieved height and  $l$  is length of the gradient.

## Acceleration resistance

The inertia of the vehicle and of all rotating parts inside the vehicle causes fictitious (d'Alembert) forces. Rotating parts are represented

$$F_a(\dot{v}) = M(1 + \delta_{eqm}) \times \frac{dv}{dt}, \quad (1.9)$$

where  $\delta_{eqm}$  is the vehicle equivalent moment inertia representing the rotating parts such a wheels and powertrain inertia.

## Demanded power

Due to analysis of performing forces acting on the vehicle body in motion for longitudinal direction the power balance can be expressed

$$\begin{aligned} P_D(t) &= f_{P_D}(v, \dot{v}, M, \phi) = (F_r + F_w + F_g + F_a)v \\ &= \left[ \frac{\rho}{2} A_f c_d v^3 + M g (c_r + \cos(\phi) + \sin(\phi)) v \right] + M(1 + \delta_{eqm}) \dot{v} v, \end{aligned} \quad (1.10)$$

## Demanded power based on position

According to data given in GPS format and with use of 3D-maps is more suitable to compute demanded power dependent on position. Therefore the equation 1.10 based on time can be transferred using the condition

$$v = \frac{ds}{dt}$$

$$\frac{dv}{ds} = \frac{dt}{ds} \frac{dv}{dt} = \frac{1}{v} \frac{dv}{dt}, v \neq 0$$

$$P_D(s) = \frac{\rho}{2} A_f c_d v^2 + Mg(c_r + \cos(\phi) + \sin(\phi)) + M(1 + \delta_{eqm})v \frac{dv}{ds}, \quad (1.11)$$

## 1.5 Components

### 1.5.1 IC engine

Parallel hybrid electric vehicle use the ICE as a prime energy source in conjunction with electric motor. This offers the ICE to work in optimal point so it can reduce emissions and reach higher efficiency, or reach better fuel consumption. When demanded power is higher than can be delivered by the engine, the power boosting from the electric motor is used.

#### Engine parameters

- Maximum rated power—the highest power for a short period that the engine is able to provide.
- Normal rated power—the highest power that is possible to deliver in continuous operation.
- Rated speed—rotational speed of the crankshaft.

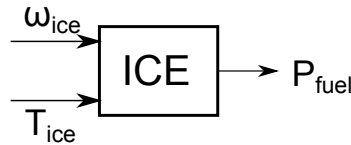


Fig. 1.11: Quasistatic model of the ICE

Globally the engine is an energy converter that converts chemical energy into mechanical. The quasistatic model is introduced in Fig.1.11, the inputs are  $\omega_{ice}$  the engine angular speed and  $T_{ice}$  the engine torque. At the output is  $P_{fuel}$  the enthalpy flow. The relationship between inputs and output is defined as

$$\eta_{ice} = \frac{\omega_{ice} T_{ice}}{P_{fuel}}. \quad (1.12)$$

Thermal efficiency mainly depends on the angular speed and torque. Function  $\eta_{ice}$  is highly nonlinear and exact description is very difficult. Another common way how to express thermodynamical efficiency is an engine map (Fig.1.12). In fact it is a look-up table indexed by the angular speed and torque, the data are generated from the steady-state engine bench tests.[10],[16]

$$P_{fuel} = m_f \times H_{LVH}, \quad (1.13)$$

where  $H_{LVH}$  is the fuel lower heating value and  $m_f$  is fuel mass flow.

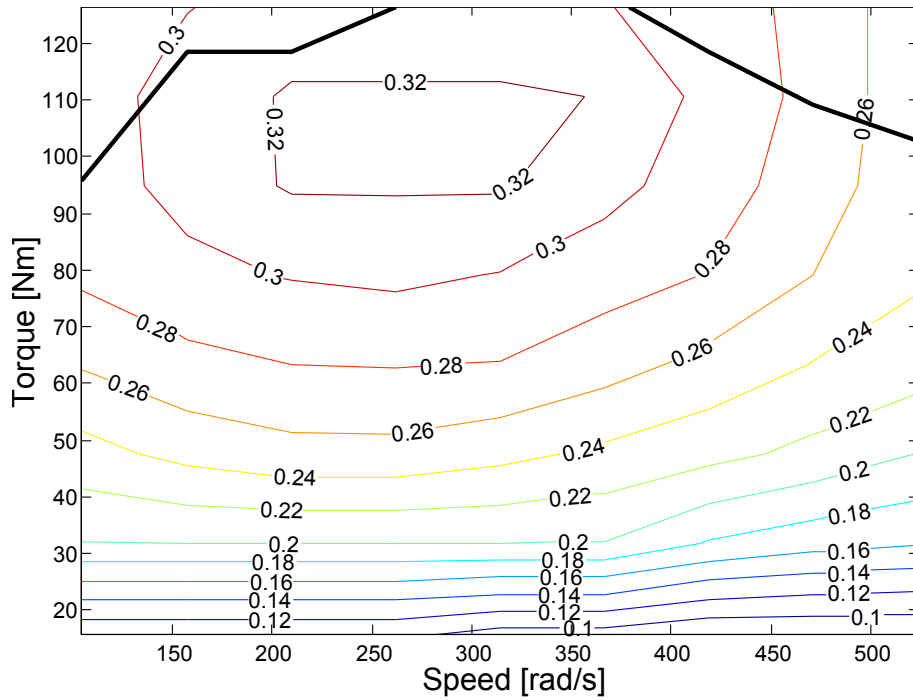


Fig. 1.12: ICE efficiency map with maximum torque curve (thick line)

## 1.5.2 Electric motor

The EM is considered as a secondary power source, but in parallel HEV architecture needs to meet a various operation modes:

- convert the electrical power from the battery into mechanical power to drive a vehicle,
- convert the mechanical power from the engine into the electrical power and charge the battery,
- recuperate the mechanical power during regenerative braking and charge the battery.

Good electric motor should offer high efficiency, low cost, high specific power, good controllability, fault tolerance, low noise and low torque fluctuations. There are

two main groups of electric motors: DC motors (permanent magnet, separately excited), AC motors (synchronous, asynchronous). DC motors-are used as a traction machines, they are simpler than the AC motors and less expensive. They do not need complicated electronic. The disadvantages are lower efficiency and the brushes, that must be changed relatively often. AC motors-are more expensive than the DC motors. They need more sophisticated control electronic, have higher power density and higher efficiency.[1],[14]

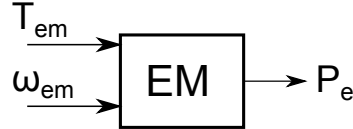


Fig. 1.13: Quasistatic model of the EM

### Motor efficiency

In quasistatic modeling the EM converts electric energy into mechanical energy and vice versa. Mechanical part represent the angular speed and torque, the output is electric power. During every conversion some energy is lost. The efficiency of conversion is defined as (1.14) when the motor works in the motor mode, and for generator mode as (1.15). Also, in this case the function  $\eta_m$  is defined by the look-up tables, thus by the efficiency maps. Some maps are measured only for motor mode, so the efficiency needs to be mirrored for generator mode as  $\eta_m(\omega_m, -|T_m|) = \eta_m(\omega_m, |T_m|)$ .

$$P_m(t) = \frac{T_m(t) \times \omega_m(t)}{\eta_m(\omega_m(t), T_m(t))}, \quad T_m(t) \geq 0, \quad (1.14)$$

$$P_m(t) = T_m(t) \times \omega_m(t) \times \eta_m(\omega_m(t), T_m(t)), \quad T_m(t) < 0, \quad (1.15)$$

where  $T_m(t)$  is the torque and  $\omega_m(t)$  is the speed required at the shaft.

### 1.5.3 Battery

Important component in all HEVs, it transforms the electrical energy into potential chemical energy during charging. During discharging converts the chemical energy into electric energy. The battery is characterized by a nominal capacity expressed in Ah, it is the number of amper-hours that could be delivered by full-charged battery until completely discharge under the certain conditions. The capacity of the battery is dependent on a discharge current rate. Another important parameters are the cycle life—number of a charging and discharging cycles before the battery starts to

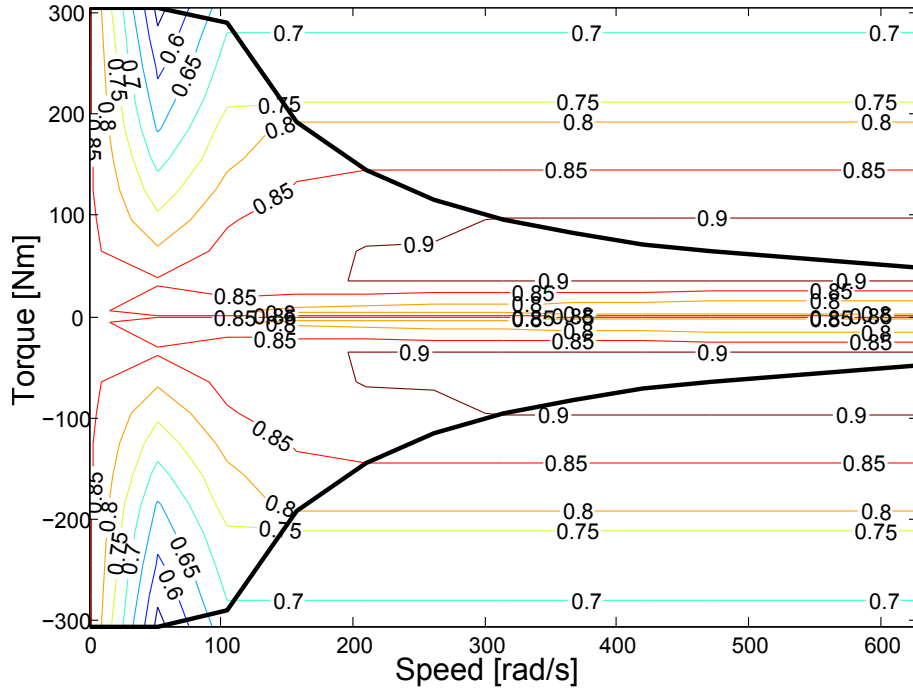


Fig. 1.14: Efficiency map for the electric motor. The thick lines represent maximal torque for given speed

lose capacity, the specific energy-amount of a useful energy that can be stored in a battery per unit mass (Wh/h), the specific power—the maximum available power per unit mass (W/kg). The quasistatic model is sketched in Fig.1.15, the input is terminal power  $P_b(t)$  and the output is battery charge  $Q(t)$ . To express a present

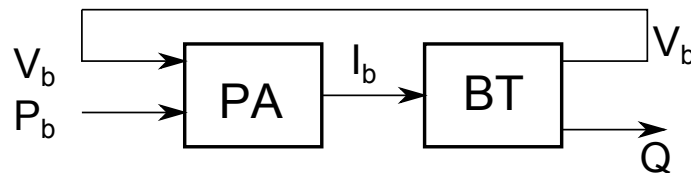


Fig. 1.15: Quasistatic model of the Battery

battery capacity is often used the term state of charge (SOC). The SOC is a ratio of the remaining capacity in the battery to the nominal battery capacity. The battery operation space is typically defined by a SOC window. The window defines minimum SOC limit that can be attained during discharge and the maximum SOC that can be reached while charge.

$$SOC(t) = \frac{Q(t)}{Q_0} \quad (1.16)$$

Direct measurement of  $Q$  is usually not possible with automotive battery system, so the variation of battery charge can be approximately related to the discharge

current  $I_b$ . [1],[16],[14]

$$\dot{Q}(t) = -I_b(t) \quad (1.17)$$

During the charge mode the current  $I_b$  is not possible to completely transformed into a charge. This effect is modeled by the Coulombic efficiency  $\eta_c$ ,

$$\dot{Q}(t) = -\eta_c \times I_b(t). \quad (1.18)$$

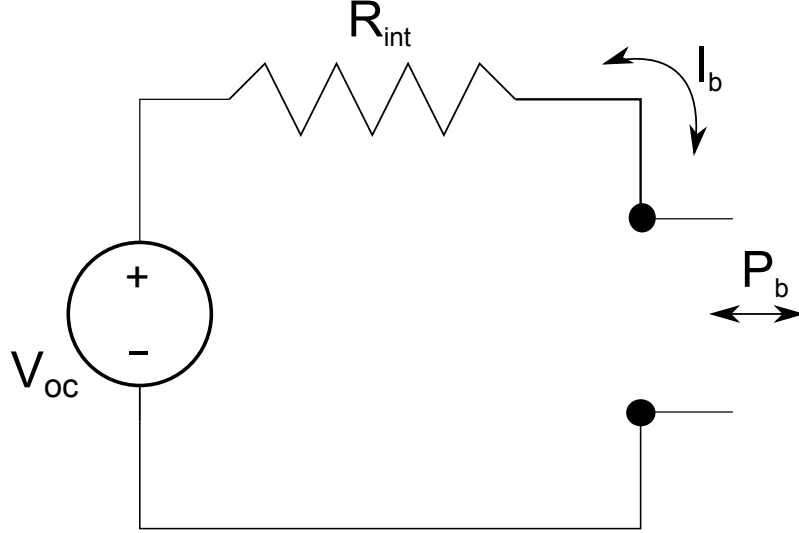


Fig. 1.16: Equivalent circuit of battery

The equivalent circuit for battery is sketched in Figure 1.16. The internal battery power  $P_{int}$  and the power at terminal  $P_b$  are described as

$$P_{int}(t) = V_{oc}(t, SOC) \times I(t), \quad (1.19)$$

$$P_b(t) = P_{int}(t) - P_{loss}(t) = V_{oc}(t, SOC) \times I(t) - I^2(t) \times R_{int}(t, SOC), \quad (1.20)$$

where,  $V_{oc}$  is the open circuit voltage and  $R_{int}$  is the internal battery resistance both are heavily dependent on the SOC as is pictured in Figure 1.17 and 1.18. The current flowing through the battery can be derived from Ohm's law as

$$I_b(t) = \frac{V_{oc} - \sqrt{V_{oc}^2 - 4 \times R_{int} \times P_b}}{2 \times R_{int}}. \quad (1.21)$$

Thus, the change of SOC during the battery operation can be expressed as

$$\frac{dSOC}{dt} = \frac{I_b(t)}{Q_0}. \quad (1.22)$$



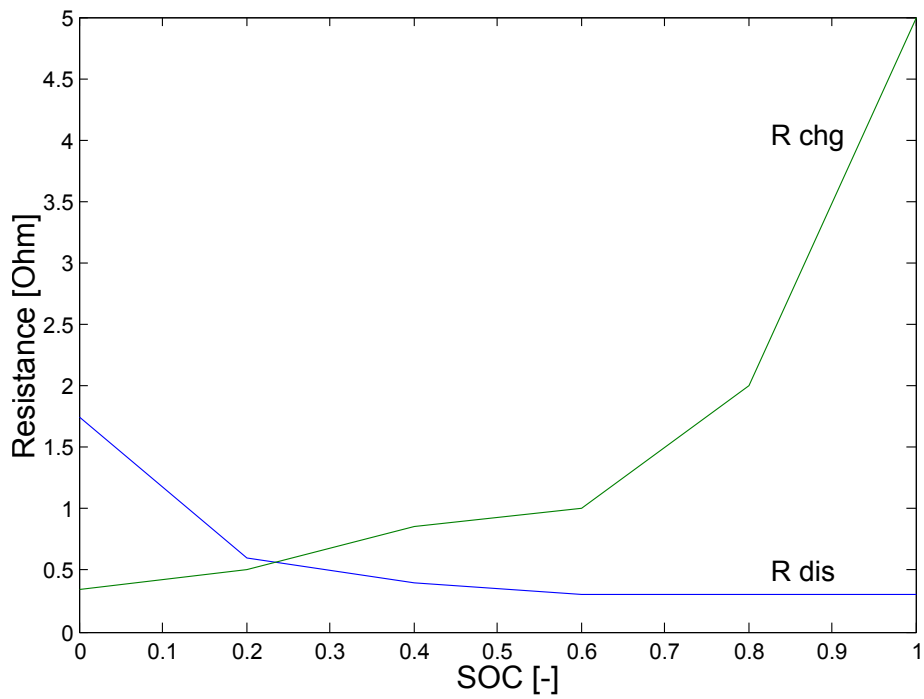


Fig. 1.17: Variation discharge and charge resistance in dependency on SOC

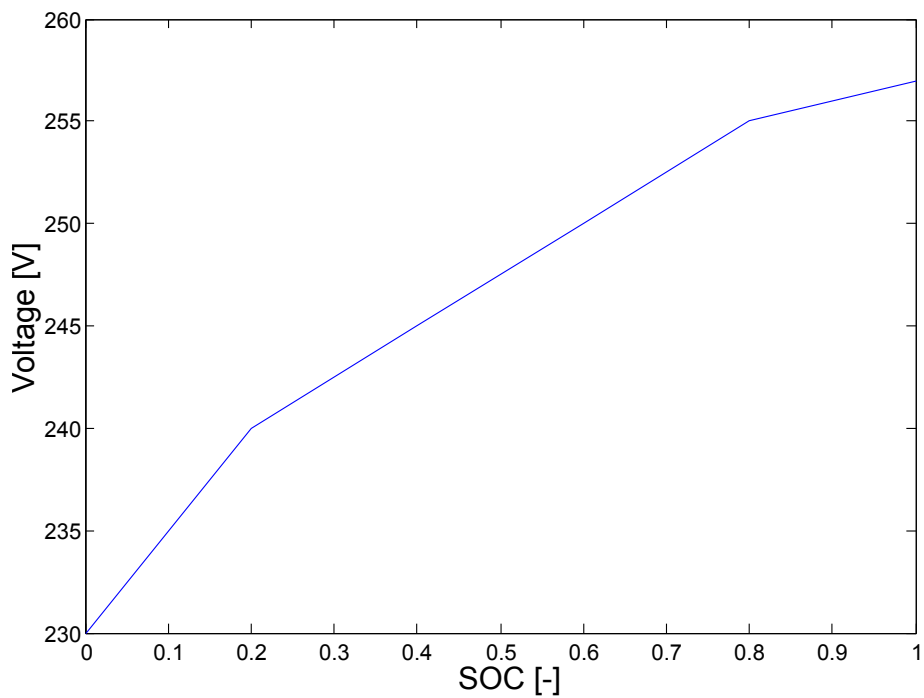


Fig. 1.18: Variation of the voltage  $V_{oc}$  in dependency on SOC

## 2 ENERGY MANAGEMENT

The main issue of the control strategy is the energy management and the load distribution between two paths in parallel hybrid car. Thus, how to reach demanded torque and achieve satisfactory fuel consumption and emissions in the same time. Also, how keep the battery state of charge on such a level to be able to delivered sufficient energy to drive the vehicle over different driving conditions. To meet this requirements the decision unit with a control algorithm is used. The inputs for the unit are globally a vehicle speed, acceleration, gear ratio and demanded torque. In some cases the inputs are extended by a road and traffic informations.

### 2.1 Classifications of control strategies

By the reason given above, various requirements have to be met during the control over the given driving cycle in parallel hybrid drivetrain. Since, the HEV's topic is popular as an option to convention vehicles, many different approaches have been introduced. Based on [11], the control strategies can be divided into: rule-based strategies and optimization-based strategies.

#### 2.1.1 Rule-based control strategies

The rules are basically designed on heuristic, human intuition and also on mathematical models. Rules are usually developed without the previous knowledge of driving cycles. Control based on rules is suitable for use in real-time control. The strategies can be classified into the deterministic and the fuzzy rule-based methods. The basic idea is to split the demanded torque among the internal combustion engine and the electric motor. In case, that the internal combustion engine is considered as a prime mover, the study [12] use the load leveling methodology to move the engine operating points into best efficiency area. The optimal operating point depends on actual request (i.e. the best fuel consumption, the best efficiency or emission). To affect the position of the operating point it requires to change the engine speed and torque, which also effect output power from the engine. Differences between the driver's torque and the torque delivered by engine has to be compensated or used by the electric motor.

**Deterministic rule-based methods** The power splitting is controlled via deterministic rules based on an analysis of power flow in the drivetrain. The simplest control method is Thermostat control strategy - method only watches over the battery high and low bounds and turning on/off the engine. Another popular solution

is Power follower control strategy - the internal combustion engine is considered as a primary power source and the electric motor producing additional power or charge the batteries by the following rules mentioned in [11].

- Below a certain minimum vehicle speed, only the EM is used
- If the demanded power is greater than the maximum power produced by the engine at its operating speed, the motor is used to compensate the difference.
- The motor charges the batteries during regenerative braking.
- The engine shuts off when the power demand falls below a limit at the current operating speed to prevent inefficient operation of the engine.
- If the battery SOC reach low bound, the engine should provide additional power to replenish the battery via the electric motor in generator mode.

However, the rules are only focused on some parts from the whole drive train and improvement in emissions is not directly taken into account. This issue tried to improve Johnson [13]. The strategy optimizes the energy usage and the emission in each operation point by applying cost function representing overall fuel consumption and emission.

**Fuzzy rule-based methods** Looking into a hybrid drivetrain as a multidomain, nonlinear and time-varying plant, fuzzy logic seems to be the most logical approach to the problem.[11] Main advantages are possibility to use this method in real-time, robustness and adaptation. The rules can be tuned depending on vehicle's components and driving cycle.

### 2.1.2 Optimization-based control strategies

Control strategy try to minimize the cost function, which represents the fuel consumption or emissions. If the optimization function is applied over all driving cycle is possible to find the global minimum of the function. To find the optimal solution the power demand over whole driving cycle is needed to know. It means to have knowledge of past and future driving condition. The cost function is given by gear ratio, torque and speed. Because this method is non-casual it can't be used as real-time control strategies. Also computational time is much longer than computation time for rule-based control strategies. However, the knowledge of those information leads to better results for the optimal torque and speed computation. Some control strategies try to solve the optimization problem in real-time so they use only information given in the exact time. The equivalent consumption minimization strategy (ECMS) proposed by Sciarretta [3] use the idea of equivalent consumption, defined as the extra fuel consumption that will be required for the battery in future time.

Results given by this methods doesn't reach the global minimum, but in [11] show that it is possible to get results very close to global minimum.

## 2.2 Drive cycle

The driving cycle carries the informations about driving conditions around the cycle. The most of cycles is defined as a set of data points representing speed with respect to time or position. The example in figure 2.1 is synthetical map with a marked route. The map is defined as a graph, the highlighted points are the vertices. Every

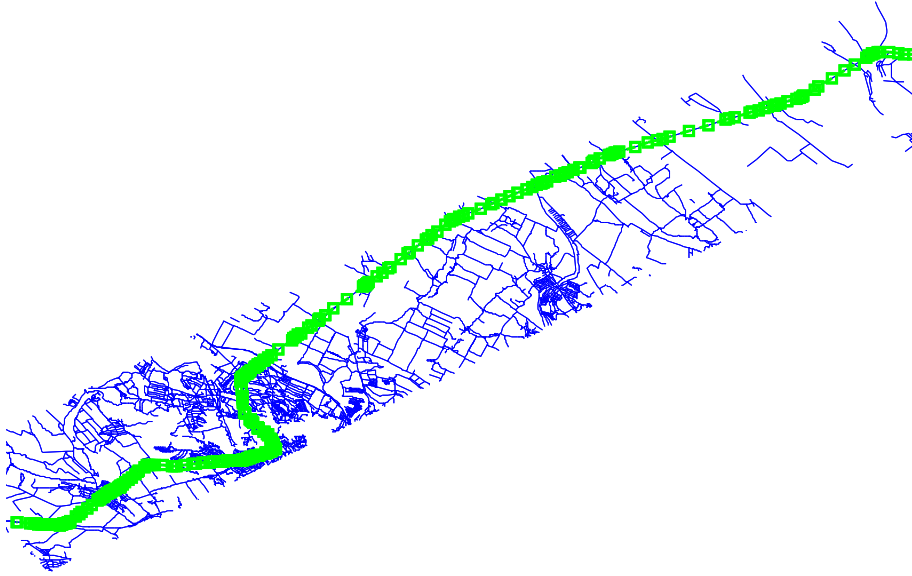


Fig. 2.1: The road in map given by vertices and edges

vertex in a route is connected with link called edge. Each vertex is defined in WGS 84 (World Geodetic System 1984) coordinates. The World Geodetic System is a standard for use in navigation and cartography. Also the GPS (Global Positioning System) works in this system. The vertices in a map are defined by the latitude, longitude and height. For the purpose of computing the power demand based on the position is more suitable to transfer the geodetic coordinates to the Cartesian coordinates as

$$\begin{bmatrix} x \\ y \\ z \end{bmatrix} = \begin{bmatrix} (N + h) \cos \varphi \cos \lambda \\ (N + h) \cos \varphi \sin \lambda \\ [(1 - e^2)N + h] \sin \varphi \end{bmatrix}, \quad (2.1)$$

where  $x, y, z$  are the Cartesian coordinates,  $\varphi, \lambda, h$  are the geodetic coordinates such latitude, longitude, height,  $N$  is the radius of curvature in the prime vertical defined

Parameter		Value
$A_f$	frontal area	2.31 m <sup>2</sup>
$\rho$	air density	1.19 kg/m <sup>3</sup>
$M$	vehicle total mass	1680 kg
$C_d$	Reynolds coefficient	0.32 kg/m <sup>3</sup>
$r_w$	wheel radius	0.29 m
$\mu_r$	rolling resistance coefficient	0.0072
$\delta_{eqm}$	equivalent moment inertia	0.195 kg/m <sup>2</sup>

Tab. 2.1: Numerical values of vehicle parameters

as

$$N = \frac{a}{\sqrt{1 - e^2 \sin^2 \varphi}} = \frac{a^2}{\sqrt{a^2 \cos^2 \varphi + b^2 \sin^2 \varphi}}, \quad (2.2)$$

where  $a, b$  are the semi-major and semi-minor axes of the ellipsoid,  $e^2$  is first eccentricity squared

$$e^2 = 1 - \left(\frac{b}{a}\right)^2. \quad (2.3)$$

Because the distance isn't constant between the vertices, the route is discretized into  $N$  segments. The discretization step is  $\Delta s = 20\text{m}$ . For each segment the velocity is interpolated and the driving condition are assumed to be constant. From the equation 1.11 is possible to derive power profile for such a route. The numerical values which define the vehicle are introduced in table 2.1, this values are used for all driving cycles. In the figure 2.2 is introduced the speed profile for a part of whole route and in figure 2.3 is plotted the demanded power over the route.

Another suitable option how to test the efficiency of energy management is use the official driving cycles developed due to needs to compare the emissions for different vehicles based on the same principle. There are a various types of driving cycles designed for different goals. In some cases the driving cycle is focused to test the fuel consumption or the polluting emission. Also the driving cycles differs by places where they are used. In European Union are preferred the cycles derived theoretically figure (2.4) the others are based on direct measurement of driving figure (2.6).

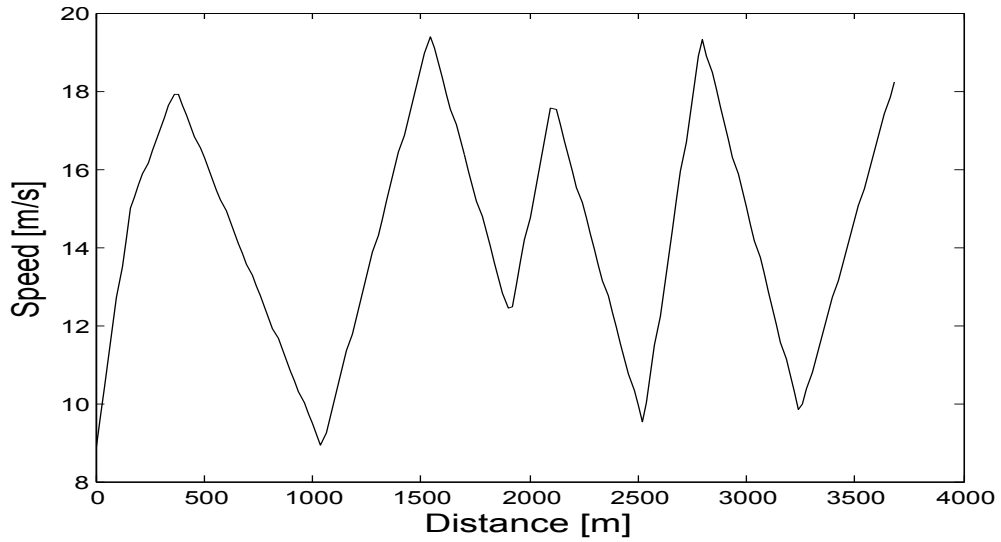


Fig. 2.2: Speed profile for given road

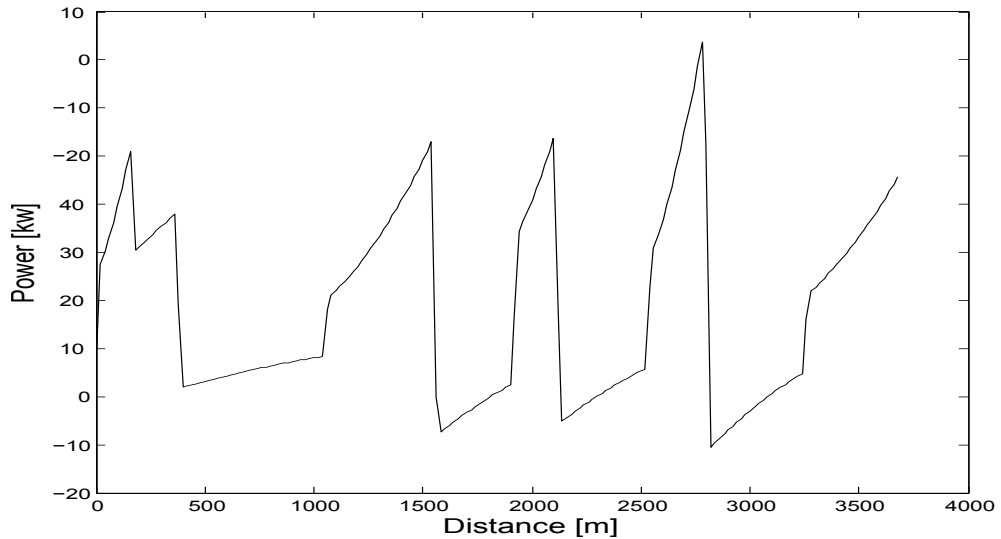


Fig. 2.3: Power profile for given road

Each driving test gives the information about a speed and a gear ratio with respect to the time. A trained driver is employed to follow the driving cycle on the chassis dynamometer. Some tests are used for a light-duty vehicles and some for a heavy-duty vehicles. The driving cycle can be divided into a steady-state cycles and a transient cycle based on the speed and load changes. The steady-state cycles consist a sequence of a constant speed and load. In the transient cycles the vehicle speed and load changes very often. To test the power management of HEV are more suitable the transient cycles. The well known driving cycle is NEDC (New European Driving Cycle) developed in European Union for testing light-duty vehicles.[15]

The NEDC contains constant acceleration, deceleration and constant speed pe-

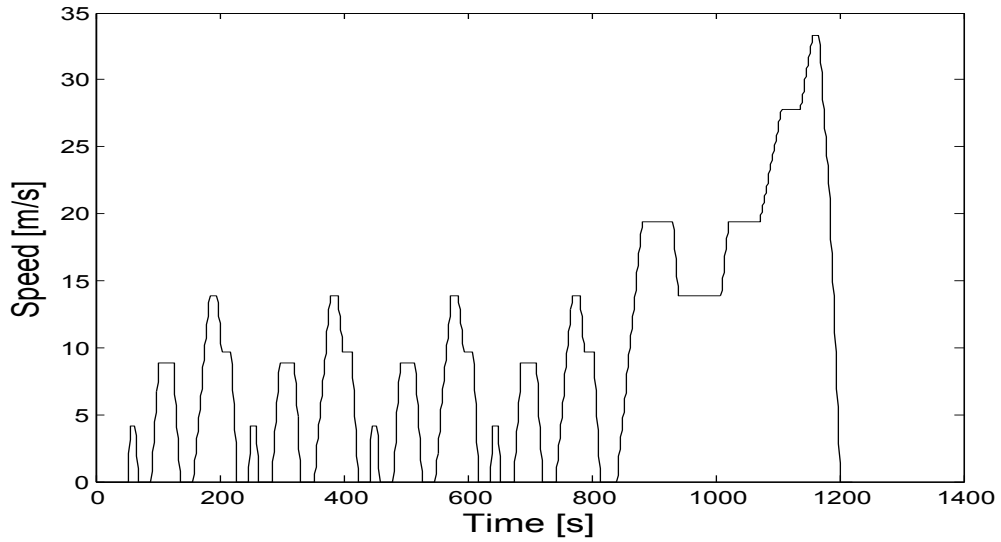


Fig. 2.4: Speed profile for New European Driving Cycle

riods. It is composed by four repeats of a low speed urban cycle (0 - 800 *s*) and a highway driving (800 - 1200 *s*). Other driving cycles for example the Federal test procedure commonly known as FTP-75 (used in United States of America) try to use real-world data. The cycle contains many speed and load variations typical for on-road driving. Globally, real-world driving cycle is more transient than stylised cycle.

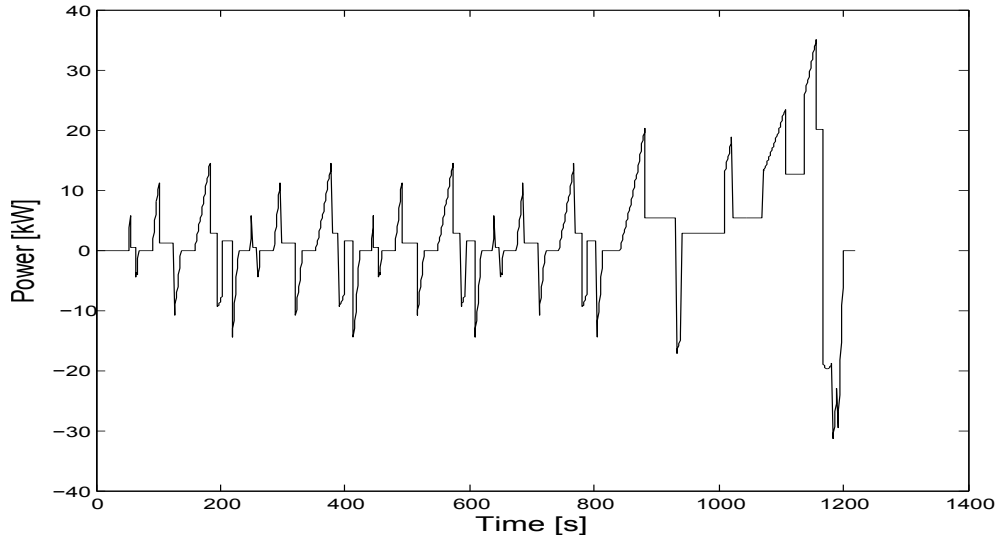


Fig. 2.5: Power profile for New European Driving Cycle

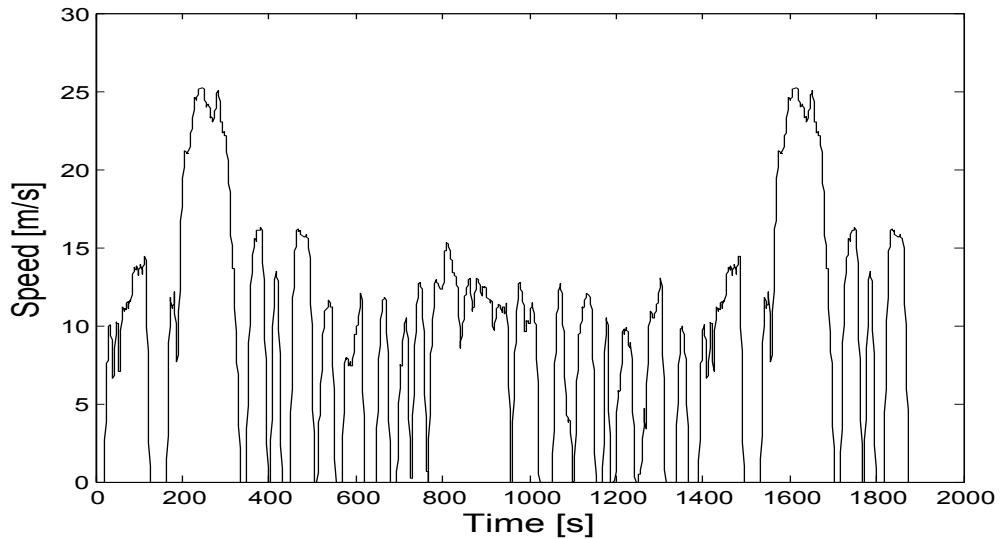


Fig. 2.6: Speed profile for FTP-75

### 2.3 Rule-based control strategy in parallel hybrid vehicle

The main idea behind this control strategy is a methodology called load leveling. The method is used in a drivetrain with the internal combustion engine as a main power source. The load leveling force the ICE to work in point with the best fuel or emission efficiency in each time over a driving cycle. It moves the operating points as close as it possible to some predefined value (Fig. 2.8). There is the vehicle speed, the torque and the gear ratio which affect the operating points of the ICE. The control strategy should not affects the driving conditions. When the speed is



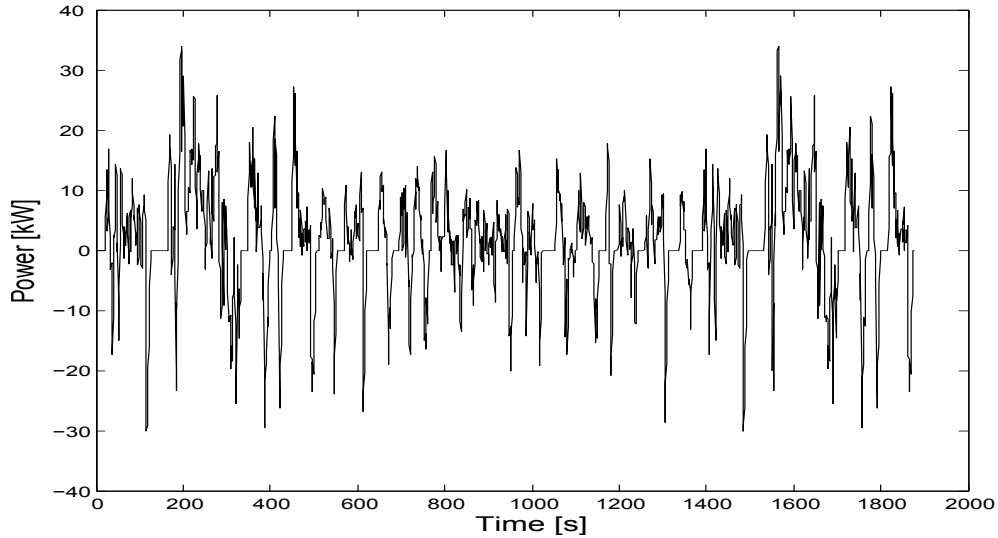


Fig. 2.7: Power profile for FTP-75 driving cycle

given by driver, the best option how to change the operating point is control the engine torque. The change of torque affects the output power from the engine. To compensate the changes of the ICE output power and to meet the demanded power is used the electric motor. The EM has globally much better efficiency than the ICE and in the ICE-dominated hybrid case doesn't affect much the global efficiency of a drivetrain. Thus, the EM plays important role in hybrid drivetrain. The motor operates in two different ways in first case the best operating point for ICE is determined, but the output power isn't sufficient to drive the vehicle and EM must produce extra power given by 2.5 it is called motor assist mode. In second case the output power of ICE is greater than demanded power or the engine needs some extra load to move the operating point so the electric motor has to act in generator mode. Extra power produced by the engine is transferred and saved in the batteries. Limitation for the electric motor are given by the SOC of battery packet, because it is desirable to keep the SOC level in prescribed boundaries. The battery shouldn't be completely discharged (if the SOC reaches the lower bound the positive torque output from EM will not be possible) or overcharged (if the battery is completely charged the EM cannot be allowed to operate as a generator). The ICE optimum estimator determines the optimal operating point given by engine speed and torque. Concrete value is dependent on the control strategy. In order to assure the necessary engine speed, proper gear ratio needs to be chosen. The optimum estimator is based on the ICE, EM and battery efficiency maps stored in lookup tables. The control unit determines the actual load of the vehicle as seen by powertrain. It has to be provided with vehicle information such as frontal area, drag coefficient, coefficient of rolling resistance, wheel radius, gear ratios and total vehicle mass.[12] At a given

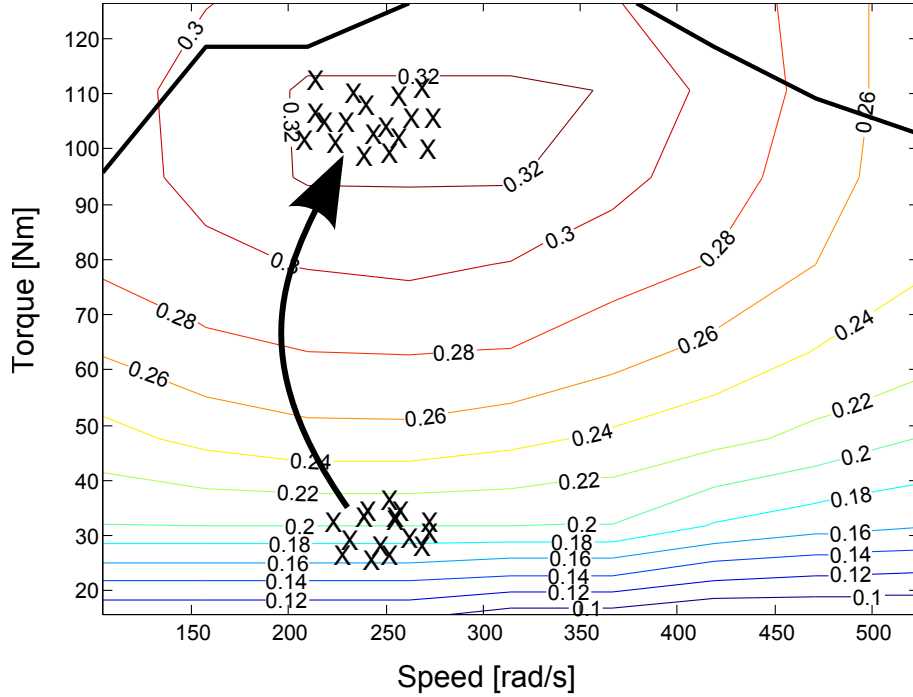


Fig. 2.8: ICE efficiency map with operating points.

speed, the power equation relates to load torque that can be computed according to

$$T_{LOAD} = T_R + T_D + T_A + T_G + T_T, \quad (2.4)$$

where

$T_R$  torque caused by the rolling resistance,

$T_D$  torque caused by the aerodynamic drag,

$T_A$  torque caused by the acceleration,

$T_G$  torque caused by the vehicle going uphill or downhill,

$T_T$  torque caused by a tow load.

$$T_{EM} = T_{LOAD} + T_{ICE}. \quad (2.5)$$

Let have a situation, when a load is too high that shifts operating point over the best efficiency area and a speed is too low to reach this area. To modify this situation, the accelerator command for ICE must decrease. While the command is executed there is not sufficient torque to overcome the road load. Than the EM needs to start working in motor mode to balance a deficit.

There are three main stages which can happen during drive cycle[18][12]:

- $0.55 < \text{Batt\_SOC} < 0.7$  - the energy level of battery is in optimal zone and it can deliver stored energy, requesting torque is checked by maximal EM torque, the flow chart is in figure 2.9,

- $Batt\_SOC < 0.55$  - energy storage is out of range, this means it must be charged. Only engine will be used to propel vehicle and charge the battery the flow chart is in figure A.2,
- $0.55 < Batt\_SOC < 0.57$  &  $flag = true$  - during driving in this range EM works mainly in generator mode to recharge the battery on the predetermined value in optimal zone, the flow chart is in figure A.3.

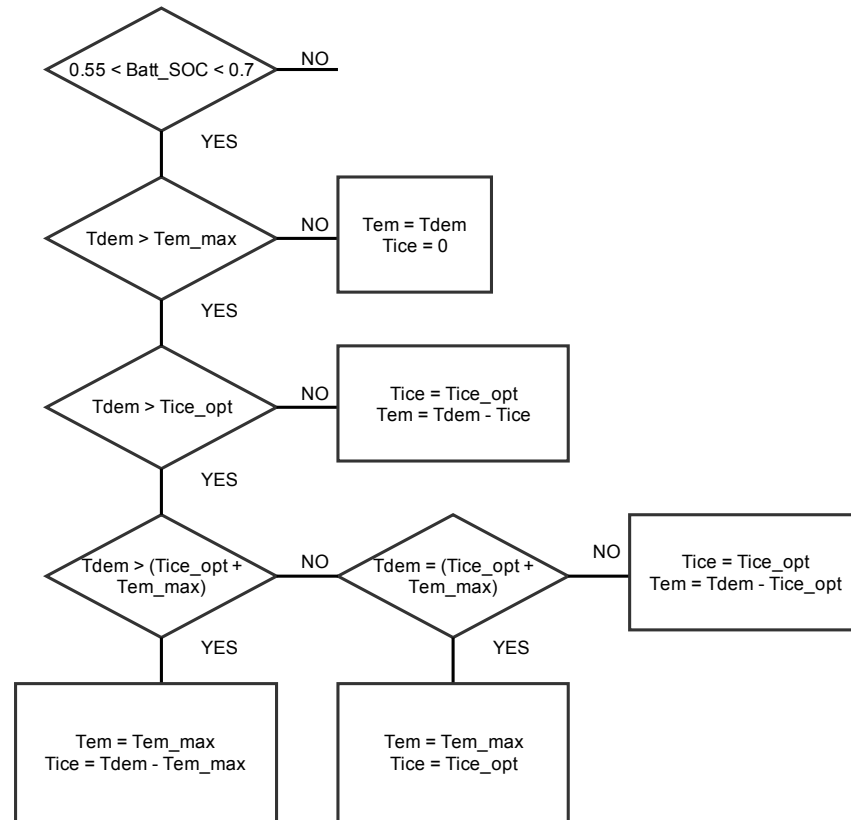


Fig. 2.9: Flowchart for  $0.55 < Batt\_SOC < 0.7$

Figure 2.10 introduces the SOC variation for FTP-75 driving cycle, the SOC trajectory starts at 0.6 and ends around 0.595. The battery is several times discharged to the lower bound, which is not desirable regarding the battery cycle life. When the SOC reaches the lower bound (0.55) the control unit switch into the third mode and charges the battery until  $SOC = 0.57$ . The results of splitting control are introduced in Fig. 2.12 for the fuel path and in Fig. 2.13 for the electric path. As one can see in Fig. 2.11, control forces the ICE operating point to be as close as it possible to the highest point of efficiency.

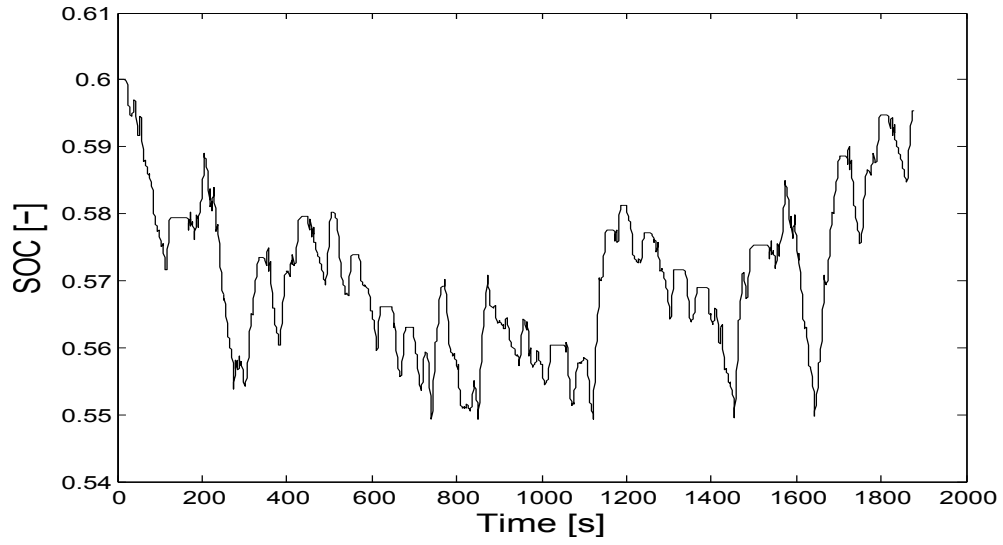


Fig. 2.10: SOC variations for FTP-75 driving cycle

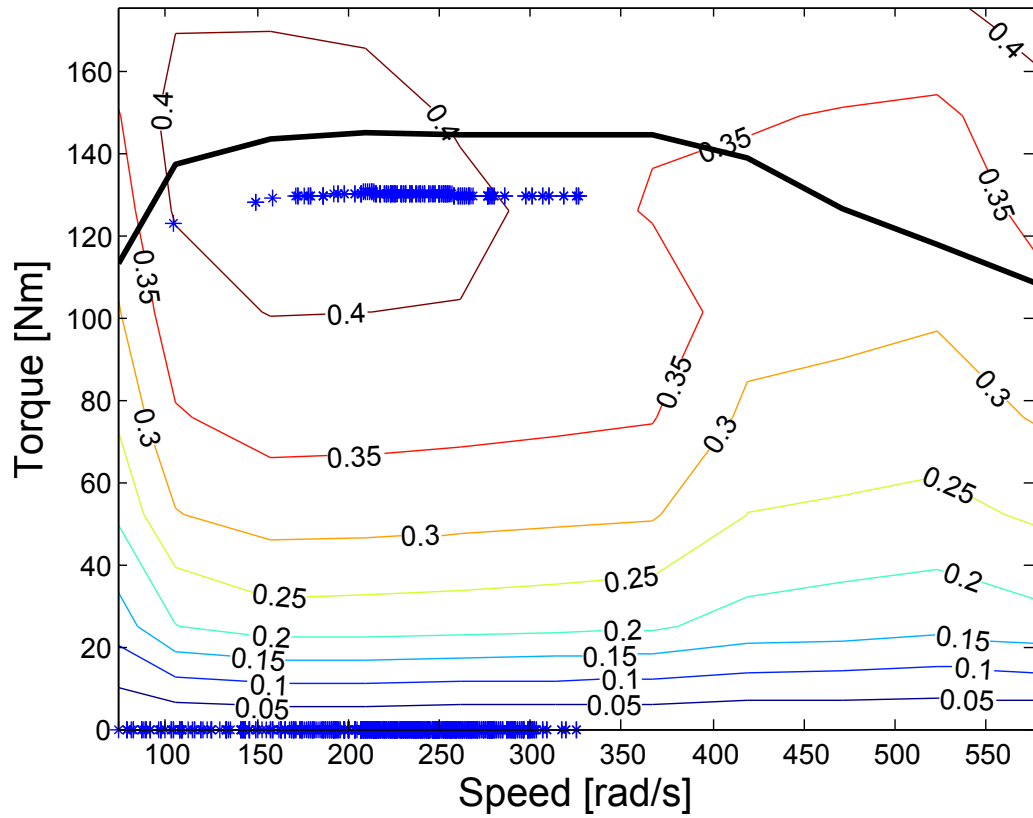


Fig. 2.11: Engine efficiency map with operating points

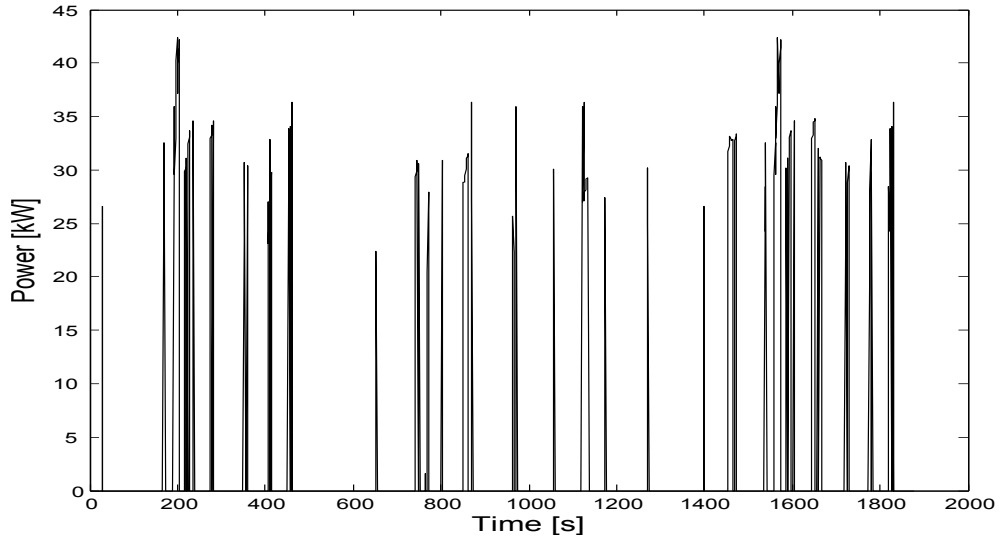


Fig. 2.12: Power trajectory in fuel path for FTP-75 driving cycle

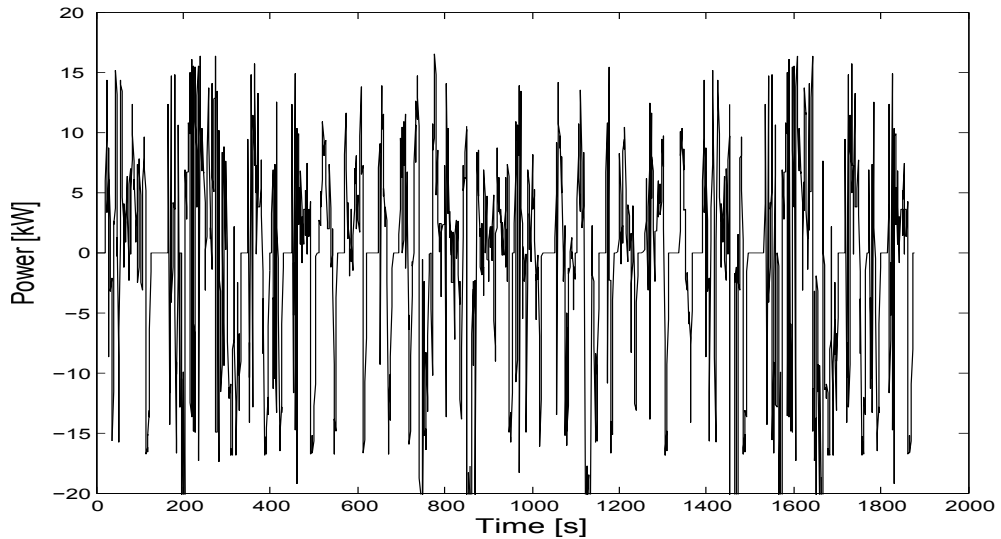


Fig. 2.13: Power trajectory in electrical path for FTP-75 driving cycle

## 2.4 Equivalent consumption minimization strategy

Parallel hybrid vehicle can be characterized as a group of inputs, control inputs, measurable outputs and state variables. The main input variable  $w(t)$  is a driving cycle which has to be followed by a vehicle. From the knowledge of a vehicle speed is possible to derive the speed and torque required at the wheels. Components in drivetrain must instantly delivered the demanded power. To manage whole powertrain the control input  $u(t)$  is needed. Optimization problem is defined by the variable which will be tuned over the drive cycle expressed as the performance index  $J$  and

the relevant state variables  $x(t)$  under the constrains. The simplest performance index  $J = m_f(t_f)$  is fuel mass  $m_f$  consumed over the driving cycle of duration  $t_f$ , where  $J$  can be expressed as

$$J = \int_0^{t_f} \dot{m}_f(w(t), u(t)) dt. \quad (2.6)$$

Into performance index can be variously added other variables such pollutant emissions or gear shifting, than more general expression is introduced

$$J = \int_0^{t_f} L(w(t), u(t)) dt, \quad (2.7)$$

where  $L$  combines the fuel consumption and the emission rates.

### State variables

The state variables are used to describe the dynamic system in mathematical way. They are related with powertrain subsystems. For the description of each subsystem the quasistatic modeling is used. For control parallel hybrid car is important only state of charge battery,  $x(t) \equiv \xi(t)$ . The optimal control must respect the dynamic of the state variable

$$\dot{x}(t) = f(w(t), u(t), x(t)). \quad (2.8)$$

It is necessary to keep the battery operating point in admissible boundaries during whole mission (state constrains). Also at the end of each mission the SOC needs to be as close as it possible to initial value. For the parallel hybrid vehicles only small deviations are allowed. There are two ways how to accomplish the condition. In first case are used so called soft constrains when either (positive or negative) deviations  $\xi(t_f)$  from final value  $\xi_t$  are penalized. In second way is used so called hard constrain which force  $\xi(t_f)$  exactly matches the value  $\xi_t$ . Soft constrains are used mainly in real-time optimization while hard constrains are relevant in offline simulations. To apply constrains on the final state  $\xi(t_f)$  the penalty function  $\phi(\xi(t_f))$  is added into the performance index [1]

$$J = \phi(\xi(t_f)) + \int_0^{t_f} L(w(t), u(t)) dt. \quad (2.9)$$

The hard constrains can be expressed as

$$\xi(t_f) = \begin{cases} 0, & \text{if } \xi(t_f) = \xi_t, \\ \infty, & \text{if } \xi(t_f) \neq \xi_t. \end{cases} \quad (2.10)$$

The soft constrains can be formalized as a function of difference as

$$\phi(\xi(t_f)) = \mu \times (\xi_t - \xi(t_f)), \quad (2.11)$$

where  $\mu$  is positive constant which penalizes battery use. The piecewise-linear function

$$\xi(t_f) = \begin{cases} \mu_{dis} \times (\xi_t - \xi(t_f)), & \text{if } \xi(t_f) < \xi_t, \\ \mu_{chg} \times (\xi_t - \xi(t_f)), & \text{if } \xi(t_f) > \xi_t, \end{cases} \quad (2.12)$$

is a core for an online energy management.[1]

### Local constrains

Local constrains define the operation limits for each component in powertrain. Mostly give us information about physical limits of the engine or motor, like the maximum torque and speed. Also give the operation boundaries for battery pack. This constrains are imposed on the state and control variables.

### Minimum principle

One of the way how to decrease the computation time is based on minimum principle. It tries to find the best possible control in the presence of constrains imposed on the state and input controls by eliminating the Hamiltonian. The Hamiltonian function is defined as

$$H(t, \xi, u, \mu) = L(w(t), u) + \mu \times f(w(t), u, \xi), \quad (2.13)$$

where  $t$  is continuous variable,  $L(w(t), u)$  is performance index,  $f(w(t), u, \xi)$  is function of state variables and  $\mu(t)$  is Lagrange multipliers defined as

$$\dot{\mu}(t) = \frac{\partial f(w(t), u(t), \xi(t))}{\partial \xi}. \quad (2.14)$$

The optimization problem is very complex in real applications, that is why the approximation in many cases is used. For example the parameters such as open-voltage or internal resistance are neglected. Consequently the optimization problem is reduced to searching for a constant parameter  $\mu_0$  that approximates  $\mu(t)$  for a given mission.[1]

In most practical cases the relationship between  $\mu_0$  and  $\xi(t_f)$  is monotonous and there is only one value  $\mu_0$  that ensure  $\xi(t_f) = \xi_t$ . If  $\mu_0$  is too high,  $\xi(t_f)$  will be higher than  $\xi_t$  and if  $\mu_0$  is too low,  $\xi(t_f)$  will be lower than  $\xi_t$ . [1] The proper value  $\mu_0$  is iteratively searched until the difference between  $\xi(t_f)$  and  $\xi_t$  is sufficiently small. The driving cycle is discretized into N points, in each point is the power demand computed. Than the control signal  $u(t)$  is introduced. For each control input is computed the Hamiltonian. The control input which gives a minimum Hamiltonian is chosen for a particular point. Whole process is repeated for next time point (Fig. 2.14). In the case when  $\mu$  will be considered as a constant the Hamiltonian function

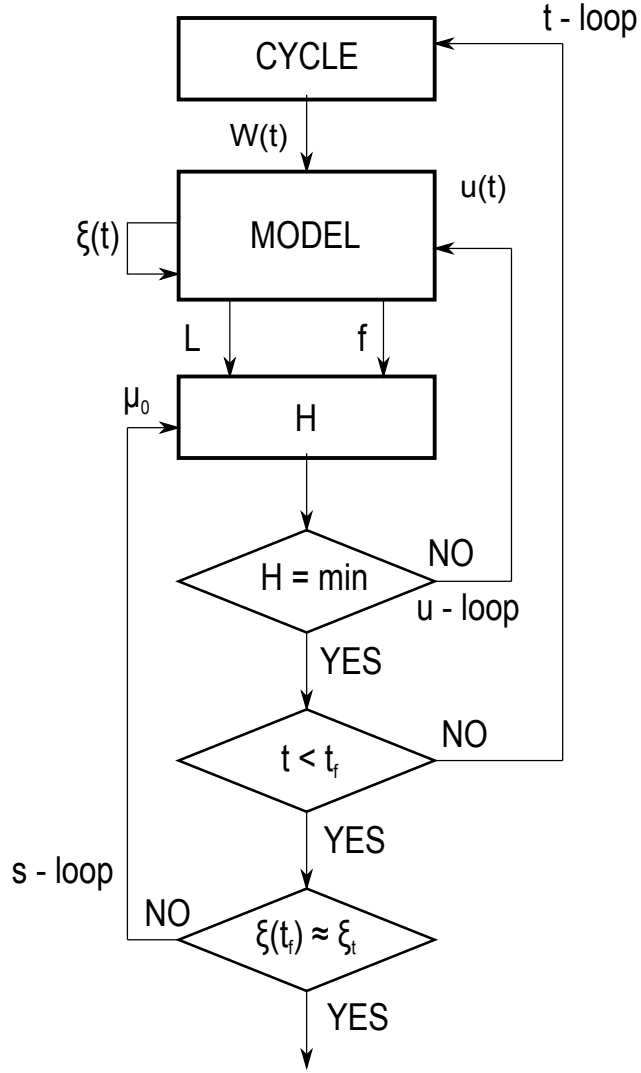


Fig. 2.14: Offline ECMS flow chart

has a new meaning

$$P_H(t, u(t), s(t)) = P_f(w(t), u(t)) + s_0 \times P_{ech}(w(t), u(t)), \quad (2.15)$$

where  $P_f$  is fuel power and  $H_{LVH}$  is lower heating value.  $P_{ech}$  is the battery electrochemical power.

$$P_f(w(t), u(t)) = H_{LVH} \times \dot{m}(w(t), u(t)), \quad (2.16)$$

$$P_{ech}(w(t), u(t)) = -\dot{\xi}(w(t), u(t)) \times U_{oc} \times Q_0 = I_b(w(t), u(t)) \times U_{oc}. \quad (2.17)$$

The equivalence factor

$$s_0 = -\mu_0 \times \frac{H_{LVH}}{U_{oc} \times Q_0}, \quad (2.18)$$

converts the battery power into an equivalent fuel consumption that is added to the actual fuel power to attain a charge-sustaining control strategy.[1] Different



approach in the power management is based on the idea, that every variation of SOC in battery pack must be compensated by engine in future. If the battery is discharged, in future will be used equivalent amount of fuel and in opposite way if the battery is charged the equivalent amount of fuel will be saved in future. The equivalence coefficients  $s_{dis}$  and  $s_{chg}$  are obtained by considering an average paths leading from fuel tank to the battery pack. What coefficient will be used is based on the discharge or charge battery status as shown

$$\begin{aligned} s_{dis} &= \frac{1}{\bar{\eta}_{chg}\bar{\eta}_{ice}}, & \text{if } E(e) > 0, \\ s_{chg} &= \frac{\bar{\eta}_{dis}}{\bar{\eta}_{ice}}, & \text{if } E(e) < 0. \end{aligned} \quad (2.19)$$

where  $\bar{\eta}_{chg}$  is the average recharging efficiency,  $\bar{\eta}_{dis}$  is the average discharging efficiency,  $\bar{\eta}_{ice}$  is the average engine efficiency. This approach allows the use of average values but during real driving the driving style and conditions changes randomly which affects efficiency of components in powertrain.

The figures introduced below show the results for energy management which use the hard constrain to accomplish the condition  $\xi(t_f) = \xi_t$ . Figure 2.15 shows the SOC trajectory for FTP-75 driving cycle. The trajectory starts at SOC=0.6 and ends at the same value as initial. Also all battery operating points are inside the SOC window. The final fuel consumption is 3.91 Liters/100 km. The demanded energy in fuel path is in Fig.2.16. Result of splitting control for electric path is in Fig. 2.16.

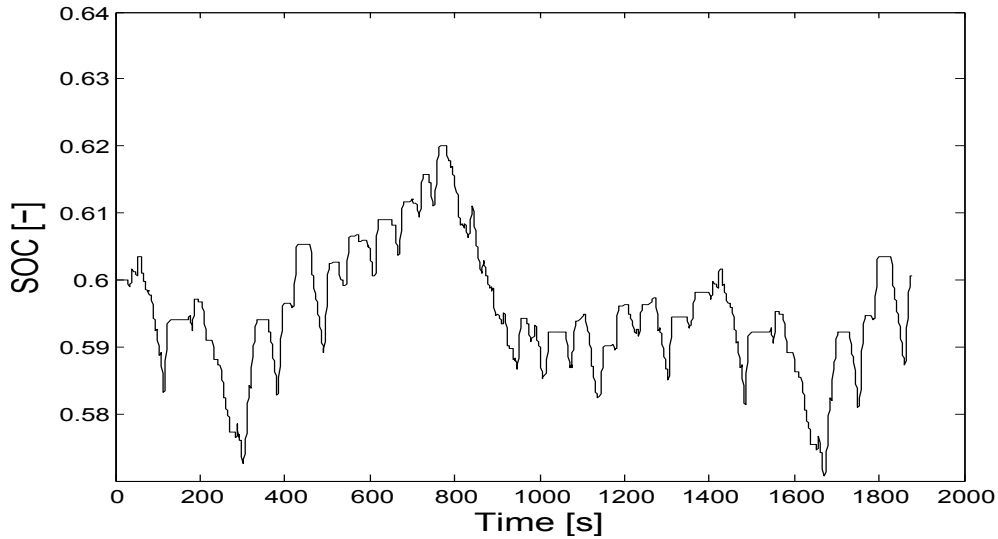


Fig. 2.15: SOC variations for FTP-75 driving cycle

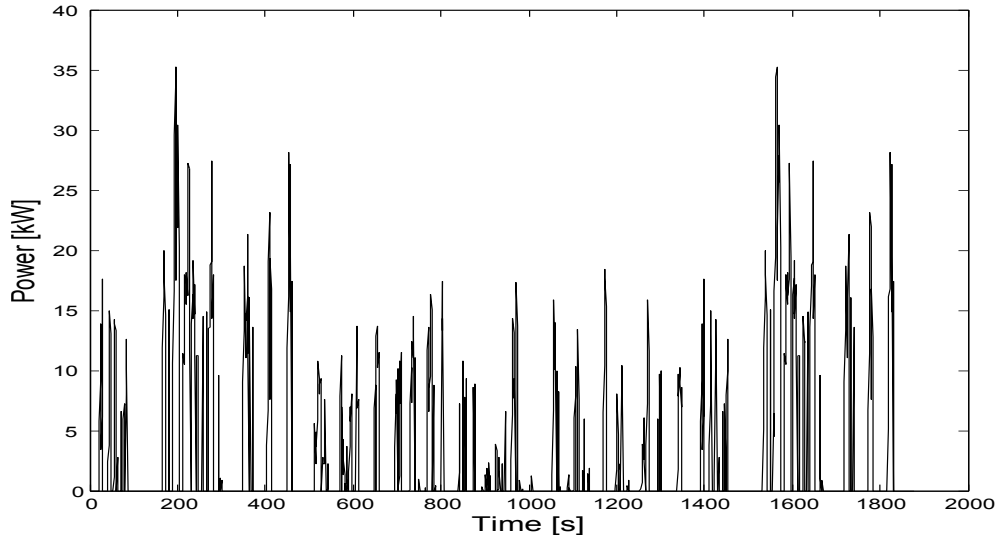


Fig. 2.16: SOC variations for FTP-75 driving cycle

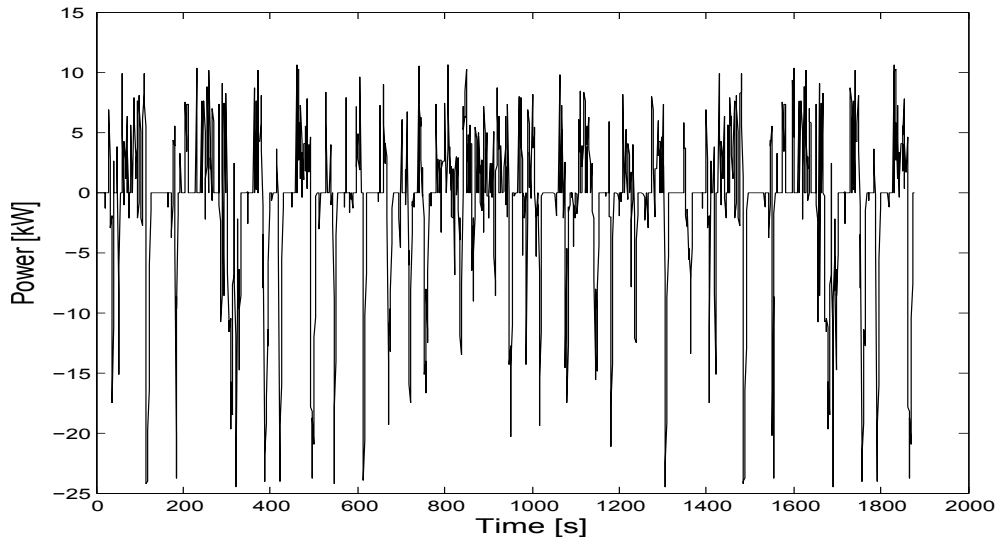


Fig. 2.17: SOC variations for FTP-75 driving cycle

## ECMS

In the case proposed by [3] is new approach how to get the equivalence coefficients between fuel and electric energy. The method sends the model of HEV through well known driving cycle with different power split ratio values  $u$  in a range  $u \in [-u_l, u_r]$  given by upper and lower bounds of SOC. The splitting ratio is constant for each driving cycle and at the end of cycle the cumulative fuel  $\bar{E}_f$  and battery  $\bar{E}_e$  energy is computed. In a case of negative power demand (regenerative braking) at the vehicle's wheels, this energy is always absorbed by electrical path. In a figure 2.18 is outlined the pure thermal mode  $u = 0$  (only engine is used to drive a vehicle) which

separates the curve  $\bar{E}_f = f(\bar{E}_e)$  in two parts which are almost linear. The slope of line for  $u > 0$  is equal to  $s_{chg}$  and for  $u < 0$  is equal to  $s_{dis}$ . Than the relationship is following

$$\bar{E}_f = f(\bar{E}_e) = \begin{cases} E_{f0} - s_{dis}(\bar{E}_e - E_{e0}), & \text{if } \bar{E}_e < E_{e0}, \\ E_{f0} - s_{chg}(\bar{E}_e - E_{e0}), & \text{if } \bar{E}_e > E_{e0}. \end{cases} \quad (2.20)$$

As was written earlier there are two parallel ways, the fuel  $T_{fpath}$  and the electrical  $T_{epath}$ , which propel a vehicle. The power demand is divided between them under the split factor  $u(t)$  as

$$u(t) = \frac{T_{epath}(t)}{T_{wh}(t)}, \quad (2.21)$$

$$T_{wh}(t) = T_{epath}(t) + T_{fpath}(t), \quad (2.22)$$

where  $T_{wh}$  is demanded torque at the wheels. When the value  $u(t) = 1$  it means that whole demanded torque will be delivered by electrical part also during regenerative braking is  $u(t) = 1$ . When  $u(t) = 0$  it is thermal mode and all demanded torque is provided by fuel part. With the given split factor it is possible to compute torque and speed of engine in every point of driving cycle by backward-facing simulation. The fuel consumption is than obtained from efficiency or fuel engine maps.[3], [21]

$$T_{ice}(t) = \frac{T_{fpath}(t)}{R_{f gb}(n(t))}. \quad (2.23)$$

$$\omega_{ice}(t) = \omega_{wh}(t)R_{f gb}(n(t)), \quad (2.24)$$

where  $\omega_{wh} = v(t)/r_{wh}$  is a speed at the wheels,  $r_{wh}$  is a wheel radius,  $R_{f gb}(n(t))$  is the engine gear ratio and  $n(t)$  is gear number. When the demanded torque from the mechanical path is known it is easy to derive torque in electrical part as

$$T_{em}(t) = \frac{T_{epath}(t)}{R_{egb}(n(t))}. \quad (2.25)$$

$$\omega_{em}(t) = \omega_{wh}(t)R_{egb}(n(t)), \quad (2.26)$$

where  $R_{egb}(n(t))$  is motor gear ratio. Similarly like in mechanical part also in electrical part are the efficiency motor maps used. The input power is derived with motor efficiency from 1.15 or 1.14 with respect to  $T_{em}$ . Than from equivalent circuit of battery the current  $I_b$  is obtained from equation 1.21. The variation of SOC battery is defined by 1.22. For control purposes the fuel energy use  $E_f(t)$ , the electrical energy use  $E_e(t)$  which is the variation of the stored electrical energy and the mechanical energy delivered at the vehicle's wheels  $E_m(t)$  are defined as

$$E_f(t) = \int_0^t \dot{m}_f(\tau)H_{LHV}d\tau, \quad (2.27)$$

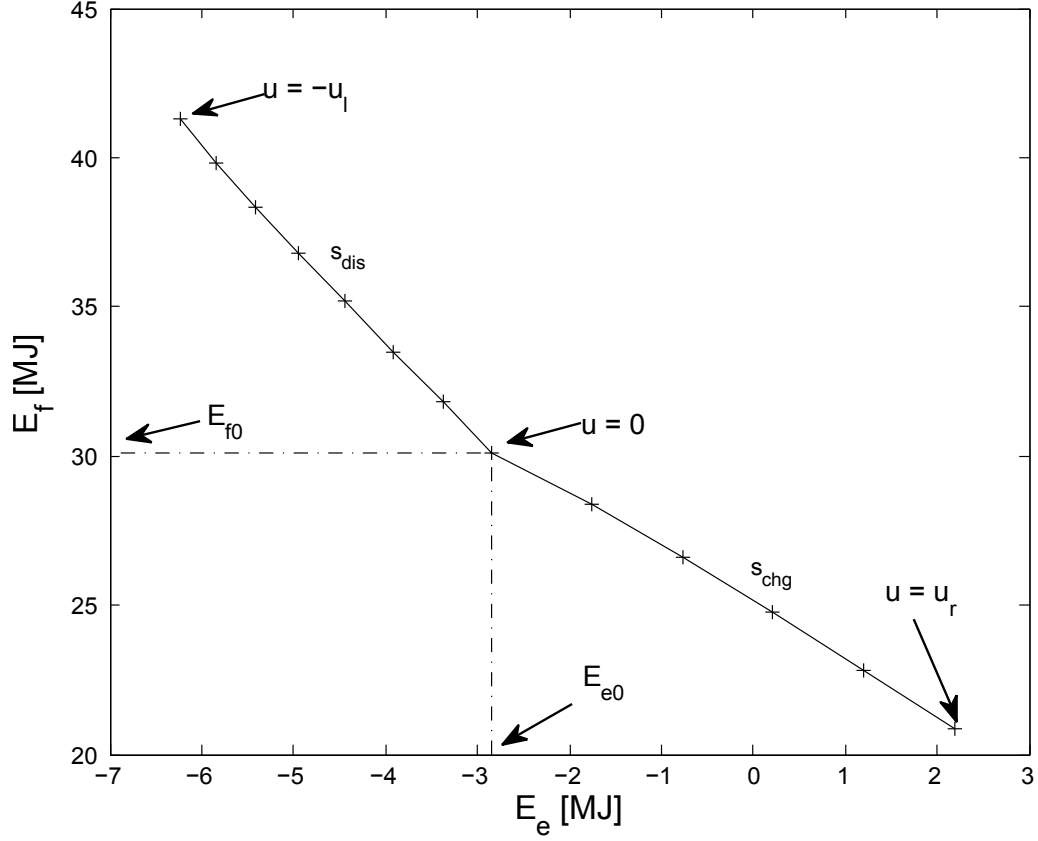


Fig. 2.18: The graph of  $\bar{E}_f = f(\bar{E}_e)$  for FTP-75 drive cycle

$$E_e(t) = \int_0^t I_b(\tau)V_b(\tau)d\tau, \quad (2.28)$$

$$E_m(t) = \int_0^t T_{wh}(\tau)\omega_{wh}(\tau)d\tau. \quad (2.29)$$

The nature of ECMS (Fig.2.19) is based on minimum principle strategy so also in this method the cost function  $J(t, u)$  is introduced as

$$J(t, u) = \Delta E_f(t, u) + s(t)\Delta E_e(t, u), \quad (2.30)$$

where  $\Delta E_f(t, u)$  is the fuel energy use and  $\Delta E_e(t, u)$  is the electrical energy use in the interval  $\Delta t$ . In each point of drive cycle is obtained such a value of control variable  $u(t)$ , which will minimize the cost function.[3] Driving conditions are assumed to be constant during  $\Delta t$ . The most important step is calculating the equivalence factor  $s(t)$ , which affects final value SOC of the battery pack. This parameter is expressed as a function  $s_{dis}$  and  $s_{chg}$  as

$$s(t) = p(t)s_{dis} + (1 - p(t))s_{chg}, \quad (2.31)$$

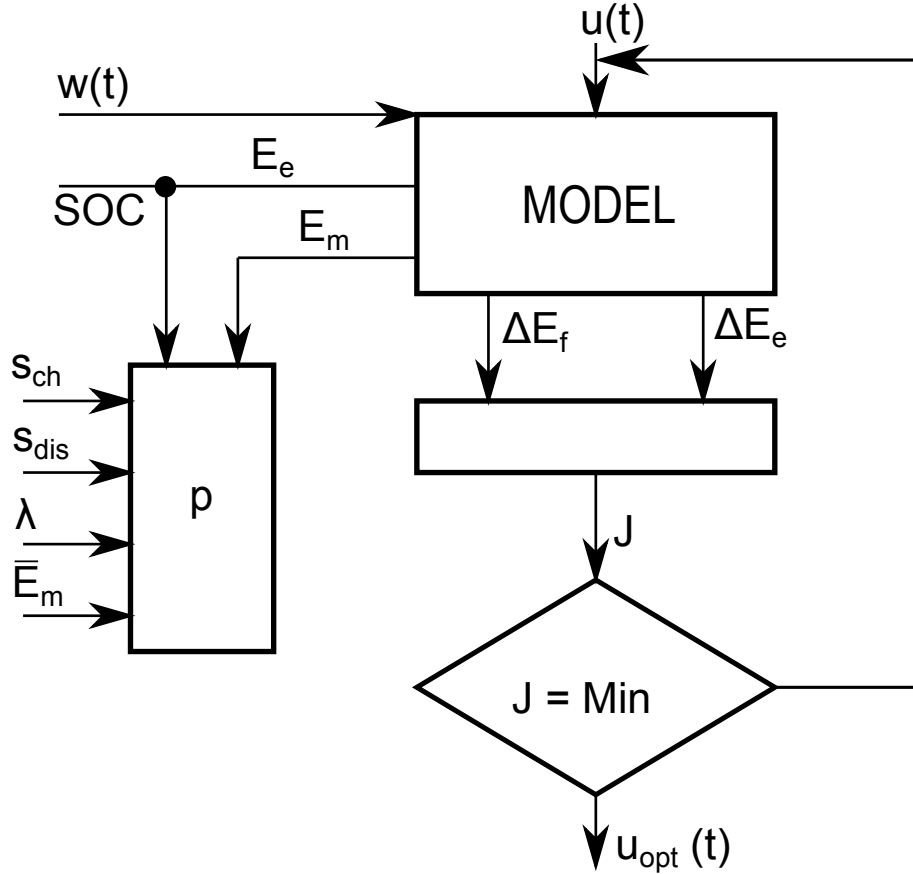


Fig. 2.19: The ECMS flowchart

where  $p(t)$  is probability that the battery will be discharged at the end of cycle if the splitting ratio  $u(t)$  will be constant until the end of drive cycle. The probability  $p(t)$  lays in interval  $[0,1]$  and is defined as

$$p(t) = \frac{u_r/\bar{\eta}_e - \lambda}{u_r/\bar{\eta}_e + \bar{\eta}_e u_l} + \frac{E_e(t)}{(u_r/\bar{\eta}_e + \bar{\eta}_e u_l)(\bar{E}_m - E_m(t))}, \quad (2.32)$$

where  $u_r$  and  $u_l$  are the upper and lower bounds of the SOC,  $\bar{\eta}_e$  is average efficiency of the electrical part defined as 2.34,  $\lambda$  is ratio of free energy and total positive mechanical energy for a whole drive cycle

$$\lambda = \frac{E_{e0}}{\bar{E}_m}, \quad (2.33)$$

$E_e(t)$  is the current value of energy in the battery and the expression  $\bar{E}_m - E_m(t)$ , tells how much mechanical energy is needed until the end of a drive cycle. The average efficiencies of fuel and electrical path can be computed with use of equivalence factors as

$$\bar{\eta}_e = \sqrt{\frac{s_{chg}}{s_{dis}}}, \quad \bar{\eta}_f = \sqrt{\frac{1}{s_{chg}s_{dis}}}. \quad (2.34)$$

The results for online ECMS energy management are pictured below. Figure 2.20 shows the SOC trajectory for FTP-75 driving cycle, the initial SOC value is 0.6 and the trajectory ends at 0.612. In compared to offline strategy small deviations from initial SOC value are present. The fuel consumption is 4.0 Liters/100 km and for pure thermal mode, splitting ratio  $u=0$ , is the fuel consumption 5.2 Liters/100 km. The equivalent coefficients were defined as  $s_{dis} = 3.24$  and  $s_{chg} = 1.49$ . The calculated values for the ratio  $\lambda$  is 0.347 and total positive mechanical energy is  $\bar{E}_m = 8.16\text{MJ}$ . Power distribution is pictured in Fig.2.21, for fuel path and in Fig.2.22, for electrical path.

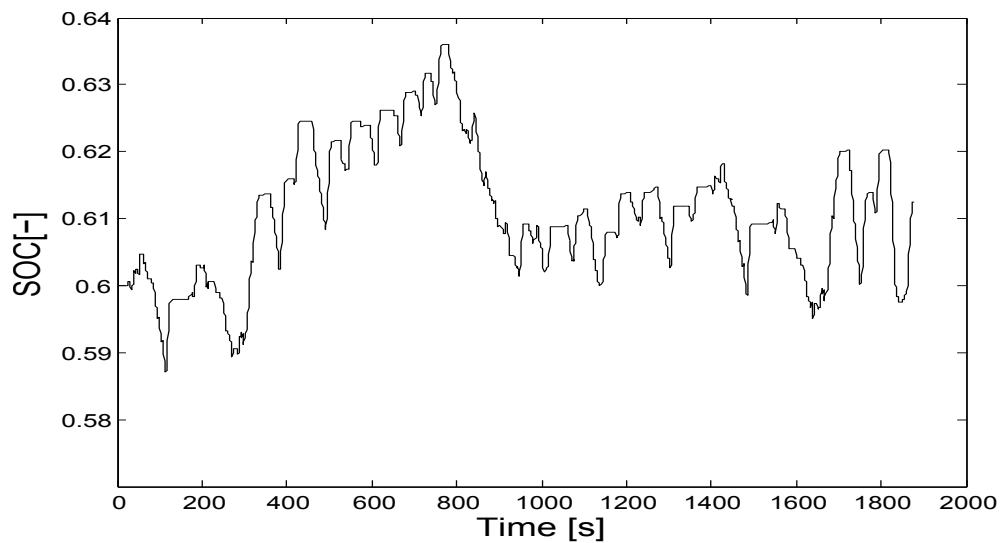


Fig. 2.20: SOC variations for FTP-75 driving cycle

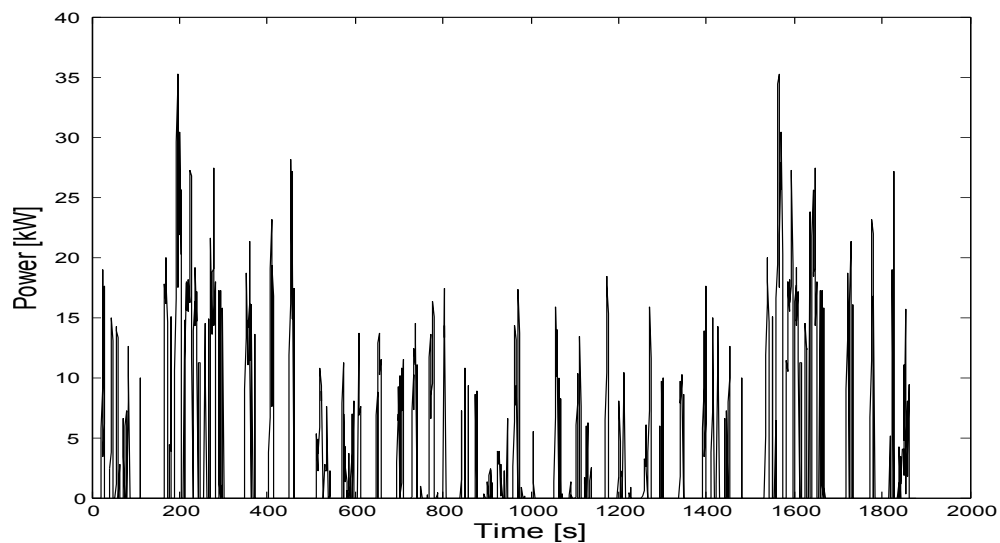


Fig. 2.21: Power trajectory in fuel path for FTP-75 driving cycle

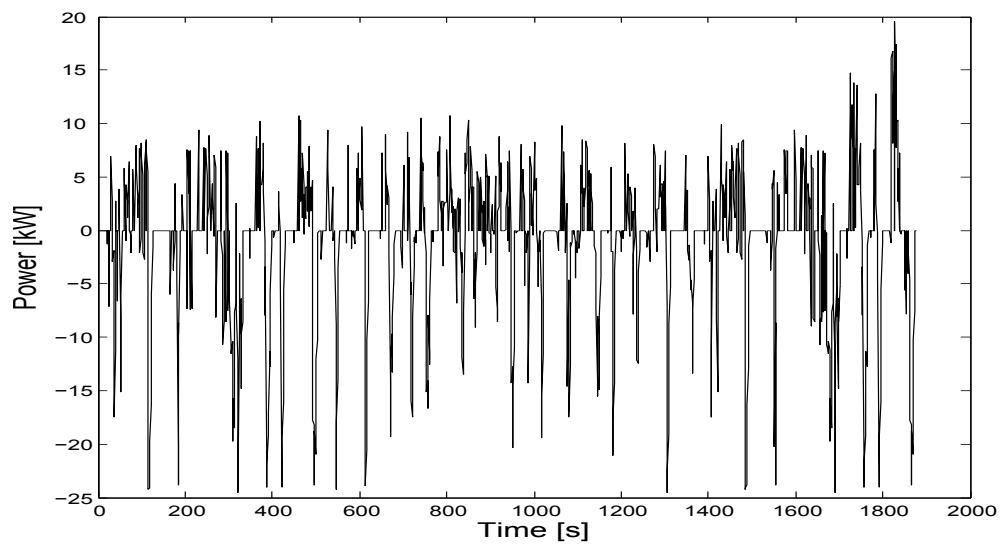


Fig. 2.22: Power trajectory in electrical path for FTP-75 driving cycle

### 3 CONCLUSION

In this work are presented and compared three energy management methods for the parallel hybrid vehicle, when the ECMS methods give a promising results. In a first part are introduced the hybrid electric vehicles. The advantages and disadvantages of main hybrid architectures are discussed. Also there is described the way how to divide the hybrid vehicles with respect to the degree of hybridization. The parallel hybrid electric vehicle is used further, that is why all operating modes are introduced. Than the mathematical description of longitudinal model is derived for the purpose of the power energy computation. The demanded power can be computed with respect to the time or position, both cases were done. To define the efficiency of whole powertrain one can use the sub-models for main components. Thus the quasi-static models for the engine, battery and electric motor are applied.

In a first section of second part the analysis of energy management strategies is introduced. Globally there are two main groups, the rule-based methods and the optimization-based methods. From the rule based methods was chosen the load leveling strategy. When all operating point of the internal combustion engine are forced to work in the most efficiency area on the particular speed. The differences are compensated by the electric motor. The idea is that the efficiency of electric motor is much higher than the efficiency of combustion engine and so the total value of lost won't be so high. From the result one can see that the operating points are very close to predefined values. But the SOC of battery was several times depleted to the lower bound of the SOC, which affects the battery life. The second method is based on the optimization strategy, when the control strategy try to minimize the cost function. The cost function in this case is represented by the fuel consumption. Thus, in each point of driving cycle is chosen the control input that satisfied minimum of cost function. To ensure that the final value of SOC will be same as initial, the hard constrain  $s = 2.315$  was used. The last method is based on equivalent consumption minimization strategy (ECMS). The ECMS uses the idea that every discharge battery will be compensated in future by higher fuel consumption and every charge battery will save the fuel in future. This method use two equivalent variables that were computed as  $s_{chg} = 1.49$  and  $s_{dis} = 3.24$ . This variables satisfy the self-sustainability of the system. Both methods improved the fuel consumption and also satisfied that the final SOC value is very close to the initial value.



## BIBLIOGRAPHY

- [1] LINO, Guzzella. *Vehicle propulsion systems: introduction to modeling and optimization*. 3rd ed. New York: Springer, 2013, p. cm. ISBN 0-8493-3154-4.
- [2] SOCIETY, Sponsors: Zhejiang University ... Technical co-sponsor: IEEE Control Systems. *2011 International Symposium on Advanced Control of Industrial Processes*. Piscataway: IEEE, 2011. ISBN 978-142-4474-608.
- [3] SCIARRETTA, A., M. BACK a L. GUZZELLA. Optimal Control of Parallel Hybrid Electric Vehicles. *IEEE Transactions on Control Systems Technology* [online]. 2004, vol. 12, issue 3, s. 352-363 [cit. 2015-05-10]. DOI: 10.1109/TCST.2004.824312. Available from: <http://ieeexplore.ieee.org/lpdocs/epic03/wrapper.htm?arnumber=1291406>
- [4] WANG, C. -L., C. -L. YIN, T. ZHANG a L. ZHU. Powertrain design and experiment research of a parallel hybrid electric vehicle. *International Journal of Automotive Technology*. 2009, vol. 10, issue 5, s. 589-596. DOI: 10.1007/s12239-009-0069-2. Available from: <http://link.springer.com/10.1007/s12239-009-0069-2>.
- [5] AGOSTONI, Stefano, Federico CHELI, Ferdinando MAPELLI a Davide TAR-SITANO. Plug-In Hybrid Electrical Commercial Vehicle: Energy Flow Control Strategies. *Advanced Microsystems for Automotive Applications 2012*. Berlin, Heidelberg: Springer Berlin Heidelberg, 2012, s. 131. DOI: 10.1007/978-3-642-29673-4\_12. Available from: [http://link.springer.com/10.1007/978-3-642-29673-4\\_12](http://link.springer.com/10.1007/978-3-642-29673-4_12).
- [6] MILLER, John M. *Propulsion systems for hybrid vehicles*. Stevenage, UK: Institution of Electrical Engineers, c2004, xvi, 455 p. ISBN 08-634-1336-6.
- [7] CHRIS MI, David Wenzhong Gao and M. *Hybrid electric vehicles principles and applications with practical perspectives*. Hoboken, N.J.: Wiley, 2013. ISBN 11-199-7011-3.
- [8] LIU, X., D. DIALLO a C. MARCHAND. Design methodology of hybrid electric vehicle energy sources: Application to fuel cell vehicles. *International Journal of Automotive Technology*. 2011, vol. 12, issue 3, s. 433-441. DOI: 10.1007/s12239-011-0051-7. Available from: <http://link.springer.com/10.1007/s12239-011-0051-7>.
- [9] LIANG, Jun-yi, Jian-long ZHANG, Xi ZHANG, Shi-fei YUAN a Cheng-liang YIN. Energy management strategy for a parallel hybrid electric vehicle

- equipped with a battery/ultra-capacitor hybrid energy storage system. *Journal of Zhejiang University SCIENCE A*. 2013, vol. 14, issue 8, s. 535-553. DOI: 10.1631/jzus.A1300068. Available from: <<http://link.springer.com/10.1631/jzus.A1300068>>.
- [10] EHSANI, Mehrdad. *Modern electric, hybrid electric, and fuel cell vehicles: fundamentals, theory, and design*. Boca Raton: CRC Press, c2005, 395 p. ISBN 08-493-3154-4.
- [11] SALMASI, Farzad Rajaei. Control Strategies for Hybrid Electric Vehicles: Evolution, Classification, Comparison, and Future Trends. *IEEE Transactions on Vehicular Technology* [online]. 2007, vol. 56, issue 5, s. 2393-2404 [cit. 2015-02-09]. DOI: 10.1109/TVT.2007.899933. Available from: <http://ieeexplore.ieee.org/lpdocs/epic03/wrapper.htm?arnumber=4305534>
- [12] BAUMANN, B.M., G. WASHINGTON, B.C. GLENN a G. RIZZONI. Mechatronic design and control of hybrid electric vehicles. *IEEE/ASME Transactions on Mechatronics* [online]. vol. 5, issue 1, s. 58-72 [cit. 2015-02-09]. DOI: 10.1109/3516.828590. Available from: <http://ieeexplore.ieee.org/lpdocs/epic03/wrapper.htm?arnumber=828590>
- [13] JOHNSON, Valerie H.; WIPKE, Keith B.; RAUSEN, David J. HEV control strategy for real-time optimization of fuel economy and emissions. *SAE Technical Paper, 2000*.
- [14] JANNEKE VAN BAALEN. *Optimal Energy Management Strategy for the Honda Civic IMA*. Eindhoven, 2006. Master's thesis. Technische Universiteit Eindhoven.
- [15] T J BARLOW a S LATHAM. *A reference book of driving cycles for use un the measurement of road vehicle emissions*. Berkshire, United Kingdom: IHS, 2009. ISBN 978-1-84608-816-2. Available from: [https://www.gov.uk/government/uploads/system/uploads/attachment\\_data/file/4247/ppr-354.pdf](https://www.gov.uk/government/uploads/system/uploads/attachment_data/file/4247/ppr-354.pdf)
- [16] ADHIKARI, Sunil. *Real-time power management of parallel full hybrid electric vehicles*. Australia, 2010. Thesis (Ph.D.). Department of Mechanical Engineering The University of Melbourne.
- [17] HUEI PENG. Comparative Study of Dynamic Programming and Pontryagin's Minimum Principle on Energy Management for a Parallel Hybrid Electric Vehicle. *Energies* [online]. Multidisciplinary Digital Publishing Institute, 2013, roč. 6, č. 4, s. 2305 [cit. 2015-05-23]. DOI: 10.3390/en6042305. Available from: <http://www.mdpi.com/1996-1073/6/4/2305>

- [18] EGHBALI, Amir Hossein, Behzad ASAEI a Peyman NADER. Fuel efficient control strategy, based on battery-ultracapacitor energy storage system, in parallel hybrid electric vehicles. *2010 IEEE Vehicle Power and Propulsion Conference* [online]. IEEE, 2010, s. 1-5 [cit. 2015-05-23]. DOI: 10.1109/VPPC.2010.5729199. Available from: <http://ieeexplore.ieee.org/lpdocs/epic03/wrapper.htm?arnumber=5729199>
- [19] SINOQUET, D, G ROUSSEAU a Y MILHAU. Design optimization and optimal control for hybrid vehicles. *Optimization And Engineering* [online]. SPRINGER, 201103, roč. 12, 1-2, s. 199-213 [cit. 2015-05-23]. DOI: 10.1007/s11081-009-9100-8. Available from: <http://link.springer.com.ezproxy.lib.vutbr.cz/article/10.1007/s11081-009-9100-8>
- [20] ZHENG, C., G. XU, S. CHA a Q. LIANG. Numerical comparison of ECMS and PMP-based optimal control strategy in hybrid vehicles. *International Journal of Automotive Technology* [online]. Heidelberg: The Korean Society of Automotive Engineers, 201412, roč. 15, č. 7, s. 1189-1196 [cit. 2015-05-23]. DOI: 10.1007/s12239-014-0124-5. Available from: <http://link.springer.com.ezproxy.lib.vutbr.cz/article/10.1007/s12239-014-0124-5>
- [21] SCIARRETTA, A. a L. GUZZELLA. Control of hybrid electric vehicles. *IEEE Control Systems Magazine* [online]. 2007, vol. 27, issue 2, s. 60-70 [cit. 2015-05-24]. DOI: 10.1109/MCS.2007.338280. Available from: <http://ieeexplore.ieee.org/lpdocs/epic03/wrapper.htm?arnumber=4140747>

# LIST OF SYMBOLS, PHYSICAL CONSTANTS AND ABBREVIATIONS

$A_f$	Frontal area [m <sup>2</sup> ]
$\rho$	Air density [kg/m <sup>3</sup> ]
$M$	Vehicle total mass [kg]
$C_d$	Reynolds coefficient [kg/m <sup>3</sup> ]
$r_w$	Wheel radius [m]
$\mu_r$	Rolling resistance coefficient
$\delta_{eqm}$	Equivalent moment inertia [kg/m <sup>2</sup> ]
$F_t$	Total tractive effort [ $N$ ]
$F_r$	Rolling resistance [ $N$ ]
$F_w$	Wind resistance [ $N$ ]
$F_g$	Climbing resistance [ $N$ ]
$v$	Speed [m/s]
$\omega$	Rotational speed [rad/s]
$T$	Torque [Nm]
$\eta$	Efficiency [-]
$m_f$	Fuel mass flow [g/s]
$H_{LHV}$	Lower heating value [J/s]
SOC	Battery SOC [-]
$I_b$	Battery current [A]
$V_{oc}$	Open circuit voltage [V]
$R_{int}$	Internal battery resistance [ $\Omega$ ]
HEV	Hybrid electric vehicle
DOH	Degree of hybridization

EV	Electric vehicle
BT	Battery
ICE	Internal combustion engine
EM	Electric motor

# LIST OF APPENDICES

A Appendix 1	55
B Content of attached CD	58

# A APPENDIX 1

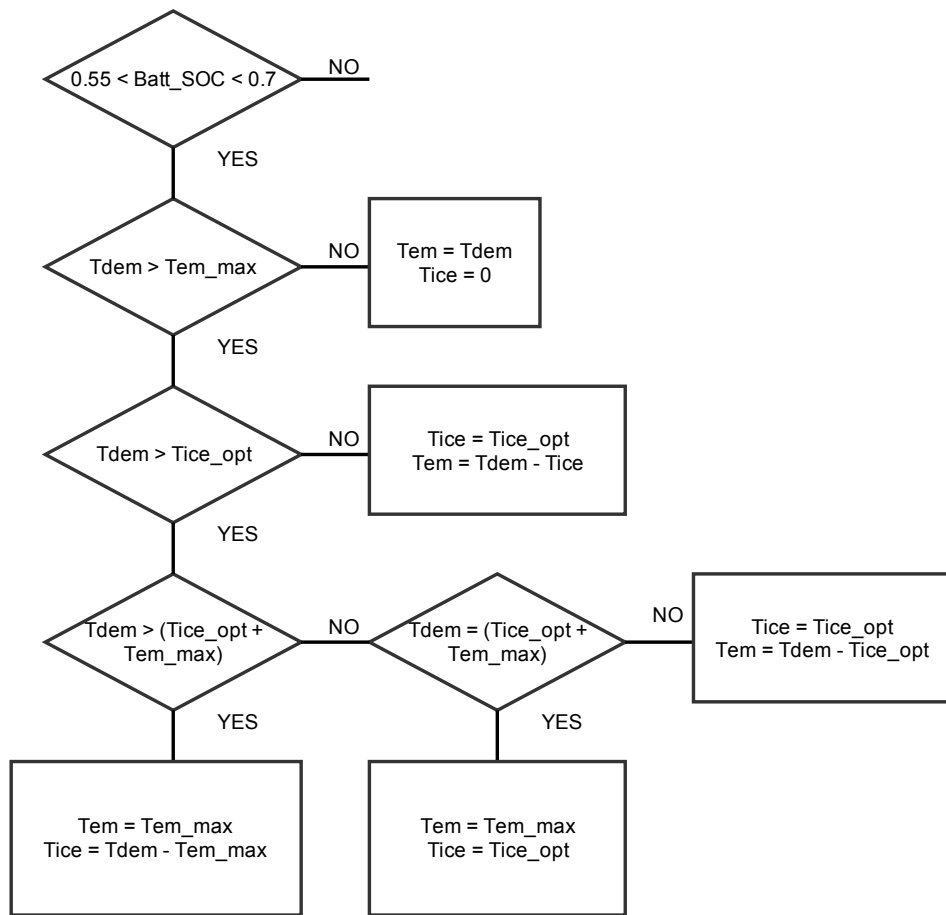


Fig. A.1: Flowchart for  $0.55 < \text{Batt\_SOC} < 0.7$

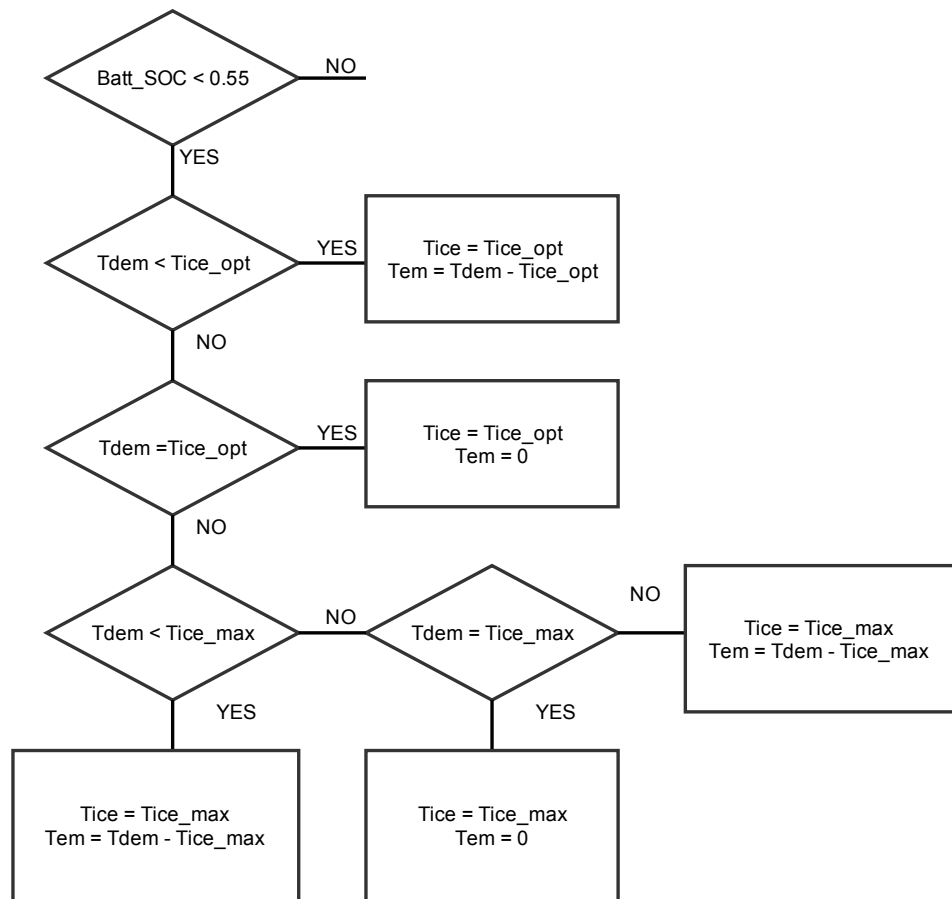


Fig. A.2: Flowchart for Batt\_SOC < 0.55



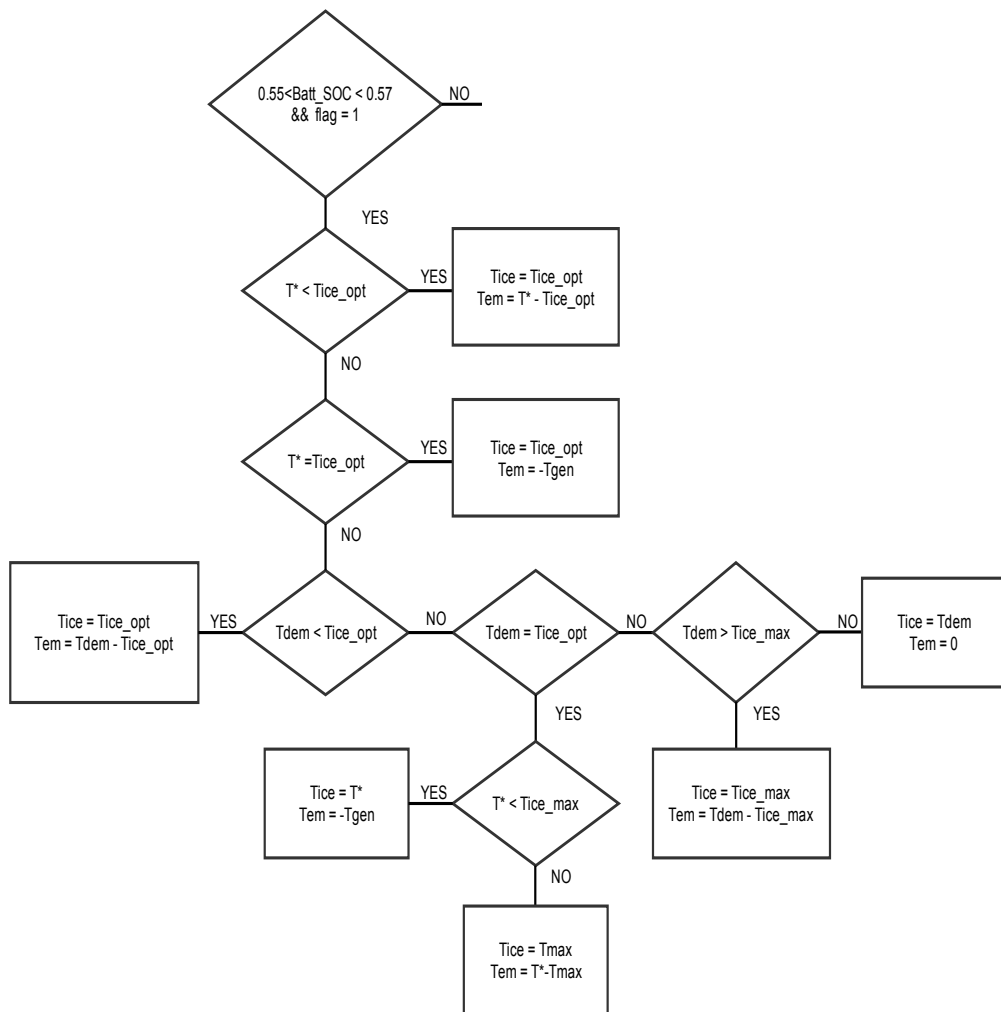


Fig. A.3: Flowchart for  $0.55 < \text{Batt\_SOC} < 0.57$  &  $\text{flag} = \text{true}$

## B CONTENT OF ATTACHED CD

The CD includes the electronic version of this work and the Matlab files for each tested method. In this work was used the Matlab 2014a version.

The folder *RuleBased* includes the *RuleBased.m* script with rule-based control strategy applied on FTP-75 driving cycle. The file *Car.m* gives the main components and variables for simulating the vehicle.

The folder *OptimizationBased* includes the *offlineECMS.m* which is control strategy based on minimum principle with hard constrains, the *onlineECMS.m* is control strategy based on ECMS both gives the splitting ratio vector that is tested in *Test.m*. The file *SlopeECMS.m* is used for finding the equivalence variables  $s_{dis}$  and  $s_{chg}$ . The file *RouteOffECMS* applies the offline ECMS strategy on route defined with respect to distance.